

## Part I

# Lecture 1: Teichmüller Theory

## 1 Bordered Surfaces

We begin with a classic geometric problem: Given a surface  $S$  describe all hyperbolic structures on the surface. For more details see [Pen06] and [FST08, FT18]

**Question 1.1.** *What kinds of surfaces are we considering?*

We will focus on **bordered surfaces with marked points**. Such a surface is classified by its genus  $g$  and number of boundary components  $b$ . We divide the marked points into two classes depending on if the marked points are in the interior or boundary of  $S$ . Marked points on the interior of  $S$  are **punctures**. Let  $p$  be the number of punctures and  $c$  be the number of marked points on the boundary. We require that at least one marked point be chosen on each boundary component.

**Question 1.2.** *What is a hyperbolic structure?*

**Definition 1.3.** *A finite area hyperbolic structure on  $S$  will be a choice of constant curvature  $-1$  metric on  $S$  with geodesic boundary arcs and every marked point (puncture or boundary) taken to a cusp.*

We consider such structures up to diffeomorphisms fixing the marked points homotopic to the identity to obtain Teichmüller space.

**Question 1.4.** *For what values of  $g, b, p, c$  is this space nontrivial?*

One version of the answer comes from Gauss-Bonnet:

$$\int_S K dA + \int_{\partial S} k_g ds = 2\pi\chi(S) \quad (1)$$

When each boundary segment is geodesic  $\int_{\partial S} k_g ds$  reduces to the sum of “turning angles” along the boundary. We are taking each marked point on the boundary to a cusp, so the “turning angle” is  $\pi$ . Thus  $\int_{\partial S} k_g ds = \pi c$ . Rearranging Equation 1 we obtain

$$\int_S K dA = 2\pi\chi(S) - \pi c = 2\pi \left( 2 - 2g - b - p - \frac{1}{2}c \right) \quad (2)$$

**Definition 1.5.** *The total curvature of a bordered surface with marked points is  $2 - 2g - b - p - \frac{1}{2}c$ .*

We write  $\chi(S)$  for total curvature of a bordered surface as a slight abuse of notation so the following theorem matches the closed surface case.

**Theorem 1.6.** *A surface  $S$  admits a hyperbolic structure iff  $\chi(S) < 0$ .*

For a closed surface ( $p = 0, b = 0, c = 0$ ) this implies  $g \geq 2$  as usual. For  $g = 1$  we need  $p \geq 1$  or  $b, c \geq 1$ . Similarly for  $g = 0$  we obtain the following table (Figure 1):

**Corollary 1.7.** *The number of triangles in an ideal triangulation of  $S$  is  $-2\chi(S) = 4g - 4 + 2b + 2p + c$*

*Proof.* This follows as the total curvature of an ideal triangle is  $-\frac{1}{2}$  (all ideal hyperbolic triangles have area  $\pi$ ).  $\square$

We will focus on non-closed surfaces. Both the triangle and punctured monogon have exactly one hyperbolic structure (there is only one ideal hyperbolic triangle up to isometry). This leads the four smallest nontrivial examples are the square (disk with 4 marked points), the punctured digon, the annulus with 2 marked points, and the once punctured torus. See Figure 2

If we want to take the next step beyond existence we will need another view of a hyperbolic structure.

$g$	$b$	$p$	$c$	$\chi(S)$	Name
0	0	3	0	-1	Thrice-punctured sphere
0	1	0	3	$-\frac{1}{2}$	Triangle
0	1	1	1	$-\frac{1}{2}$	Punctured monogon
0	2	0	2	-1	Annulus with 2 marked points
1	0	1	0	-1	Once punctured Torus
1	1	0	1	$-\frac{3}{2}$	Torus with boundary
2	0	0	0	-2	Two holed torus

Figure 1: Minimal possible negatively curved bordered surfaces with marked points

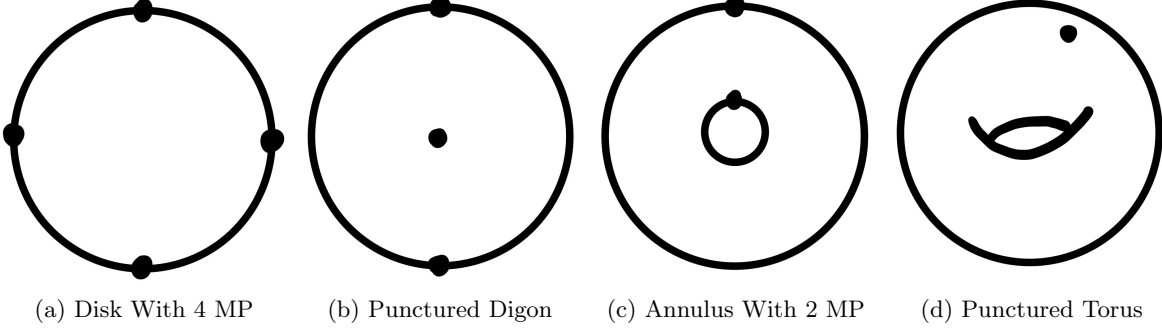


Figure 2: The smallest surfaces with a nontrivial amount of hyperbolic structures

### 1.1 Developing Map

**Definition 1.8.** An alternate definition of a hyperbolic structure on a surface  $S$  is the existence of the following pair of maps  $\text{dev}: \tilde{S} \rightarrow \mathbb{H}^2$  and  $\text{hol}: \pi_1(S) \rightarrow \text{PSL}(2, \mathbb{R})$ . We call such a pair a **developing pair**. The functions are related by the following equation for any  $\gamma \in \pi_1(S)$  and  $p \in \tilde{S}$

$$\text{dev}(\gamma.p) = \text{hol}(\gamma) \cdot \text{dev}(p)$$

For our bordered surfaces we require that each puncture and marked point is sent to an ideal point on  $\partial\mathbb{H}^2$ .

Note that developing pairs are usually considered up the action of  $\text{PSL}(2, \mathbb{R})$  by  $g(\text{dev}, \text{hol}) \mapsto (g \circ \text{dev}, g \text{hol } g^{-1})$ .

**Remark 1.9.** When the image of the developing map is all of  $\mathbb{H}^2$  we recover  $S$  as  $\mathbb{H}^2 / \text{hol}(\pi_1(S))$  and say the hyperbolic structure is complete.

**Remark 1.10.** In general the notion of a developing pair works for any target geometry  $X$  and  $G$  a group of isometries by replacing  $\mathbb{H}^2$  with  $X$  and  $\text{PSL}(2, \mathbb{R})$  with  $G$ .

**Remark 1.11.** The essential data of the developing map is the choice of boundary images of the marked points. We can define a **framed representation** to be a representation  $\rho: \pi_1(S) \rightarrow \mathbb{H}^2$  with a  $\rho$  equivariant choice of ideal points for each marked point of  $S$ .

**Example 1.12.** First we consider the disk with 4 marked points (Figure 3a). Here  $\pi_1(S)$  is trivial and the holonomy representation is trivial, so all data is in configuration of ideal points.

Recall that up to the action of  $\text{PSL}(2, \mathbb{R})$  we can send 3 points to  $0, 1, \infty$ . The last point is sent to  $x$  which we call the cross ratio of the four points.

**Example 1.13.** Now consider the annulus with two marked points (Figure 3c).

Here  $\pi_1(S) = \mathbb{Z}[\gamma]$  where  $\gamma$  is the loop around the puncture. If we fix an ideal triangulation of the annulus we can develop one triangle at a time. After two triangles we return to the same edges “up to the action of  $\gamma$ ”. As such we see that actually choice of one ideal point is forced by the representation. The next triangle has one new endpoint again determined by  $\gamma$ . From the last example we saw that one square “corresponded” to one parameter of data. In this case we have two distinct squares and remark that our triangulation has two interior edges.

**Example 1.14.** Finally we look at the punctured torus (Figure 3d).

Here  $\pi_1(S) = \mathbb{Z}[\gamma] * \mathbb{Z}[\eta]$ . If we develop triangle by triangle we observe that  $\rho$  determines the value of flags. Starting from a flag  $x$  we see the flag the other flags on the triangle should be  $\gamma.x, \eta.x$  respectively. When we had the next triangle we have a potential problem, as this flag should both be  $\gamma\eta.x$  and  $\eta\gamma.x$ . This condition is equivalent to  $\eta^{-1}\gamma^{-1}\eta\gamma.x = x$ . The path  $\eta^{-1}\gamma^{-1}\eta\gamma$  is the path around the puncture and so we see that part of the data of a framed representation is that the paths around punctures must fix the flag there.

We can count distinct squares here as well and see there are 3 choices (each square has 2 of the 3 arcs in the triangulation). Once again note this is the number of non-boundary edges of the triangulation.

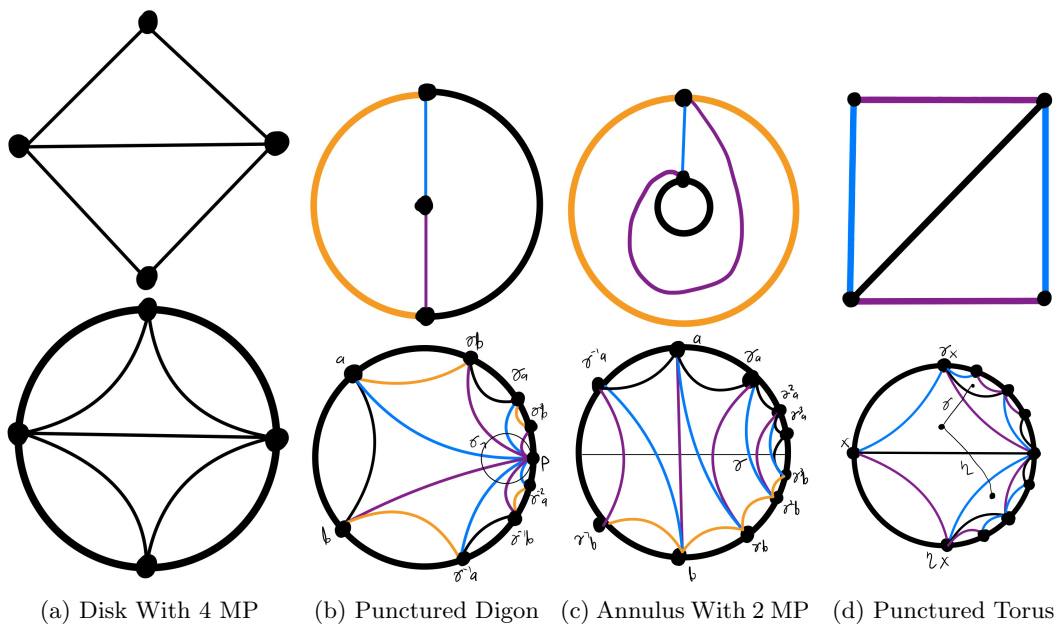


Figure 3: Developing Images Of Basic Examples

## 2 Coordinate System

The first coordinate system we consider is the “X-space”. To our surface with an ideal triangulation we can assign a set of cross ratios to each quadrilateral.

### 2.1 Cross Ratios

Recall that  $\partial\mathbb{H}^2$  can be identified with the projective line  $S^1$ . So given 4 points  $x, y, z, w \in \partial\mathbb{H}^2$  we define

$$\text{cr}(x_1, x_2, x_3, x_4) = \frac{(x_2 - x_1)(x_4 - x_3)}{(x_3 - x_2)(x_4 - x_1)} \quad (3)$$

**Remark 2.1.** *The usual cross ratio in projective geometry is  $\text{cr}(x_1, x_3, x_2, x_4) = 1 - \text{cr}(x_1, x_2, x_3, x_4)$ . One reason for this change is our choice behaves especially nicely under cyclic rotation of the points:*

$$\text{cr}(x_1, x_2, x_3, x_4) = \frac{1}{\text{cr}(x_2, x_3, x_4, x_1)} = \text{cr}(x_3, x_4, x_1, x_2) = \frac{1}{\text{cr}(x_4, x_1, x_2, x_3)}$$

Consider a square in an ideal triangulation. If we read the vertices clockwise starting from either end of the diagonal we obtain the same cross ratio  $\text{cr}(x_1, x_2, x_3, x_4)$ . As such we associate this cross ratio to the diagonal of the square.

**Lemma 2.2.** *The cross ratio is invariant under isometries of  $\mathbb{H}^2$ .*

*Proof.* One can check that Möbius transformations fix the cross ratio (suffices to check translation  $x \mapsto x + a$ , homothety  $x \mapsto bx$  and inversion  $x \mapsto -1/x$ ).  $\square$

This leads to an alternate phrasing of the cross ratio. Given four points  $(x_1, x_2, x_3, x_4)$  chose an isometry  $f$  sending  $(x_2, x_3, x_4)$  to  $(0, 1, \infty)$ . Such an  $f$  is unique as  $\text{PSL}(2, \mathbb{R})$  acts simply transitively on triples (there is only one ideal triangle!). Then

$$\text{cr}(x_1, x_2, x_3, x_4) = \text{cr}(f(x_1), 0, 1, \infty) = \frac{(0 - f(x_1))(\infty - 1)}{(1 - 0)(\infty - x_1)} = -f(x_1).$$

**Remark 2.3.** *As the action of  $\text{PSL}(2, \mathbb{R})$  preserves orientation, from this description we see that  $f(x_1) < 0$  and so the cross ratio is positive.*

**Theorem 2.4.** *An ideal triangulation on a surface determines a list of  $6g - 6 + 3p + 3b + c$  cross ratios. The values of these cross ratios for a particular hyperbolic structure, uniquely identify the structure.*

*Proof.* Recall the developing pair assigns points on the boundary of hyperbolic space to each marked point on  $S$ . As described above there is a well defined cross ratio associated to each square with diagonal. The number of these squares correspond to the number of interior arcs in the triangulation. We recall from Corollary 1.7 that the triangulation contains  $4g - 4 + 2p + 2b + c$  triangles. Note that each interior edge belongs to 2 triangles and each boundary edge belong to one triangle. We note that the number of boundary edges is  $c$ . So if  $e$  is the number of interior edges we have

$$\begin{aligned} 3t &= 2e + c \\ 12g - 12 + 6p + 6b + 3c &= 2e + c \\ 6g - 6 + 3p + 3b + c &= e \end{aligned}$$

We postpone the proof of reconstructing a representation given a list of positive real numbers associated to each interior edge to a future lecture.  $\square$

## 2.2 Changing Triangulation

One natural question is how the  $X$  coordinates change if we chose a new triangulation. Analyzing the change between two arbitrary triangulations is difficult. However there is a theorem that any two triangulations are connected by sequence of “geometric flips”.

**Definition 2.5.** A *geometric flip* at an interior edge  $e$  of a triangulation  $T$  produces a new triangulation  $\mu_e(T)$  given by removing  $e$  and replacing it with the other diagonal of the square containing  $e$ .

**Theorem 2.6.** Any two triangulations of a bordered surface can be reached by a sequence of geometric flips.

*Proof.* See [FT18] Proposition 3.8 for sources of a proof.  $\square$

Thus to understand how coordinates change we only need to understand a single geometric flip.

**Lemma 2.7.** If the edge  $e$  is replaced with the edge  $f$  in a geometric flip then the new cross ratio  $X_f = X_e^{-1}$ .

*Proof.* This follows from the analysis of the cyclic rotation of a cross ratio in Remark 2.1.  $\square$

However we see that this geometric flip changes what squares appear in the triangulation. Analyzing the way these neighboring cross ratios change is difficult. Instead we will add some information to the hyperbolic structure. This will allow us to define a related coordinate system which we can use to understand the  $X$  coordinates.

## 3 Decorated Teichmüller Space

**Definition 3.1.** A *decoration* of a hyperbolic structure on a bordered surface  $S$  is a choice of horocycle for each marked point of  $S$ .

Recall that informally a horocycle is the set points “equidistant” from an ideal point called the center of the horocycle. Formally a horocycle is a curve whose normal directions all limit to the same ideal point. In the Poincare Disk model horocycles correspond to circles tangent to the boundary at the ideal point. Similarly in the upper half plane model horocycles are circles tangent to the x-axis or horizontal lines for horocycles centered at infinity.

It is instructive to think about horocycles in the hyperboloid model as well. Here ideal points correspond to lines in the asymptotic cone. Given such an ideal point  $\lambda(x, y, \sqrt{x^2 + y^2})$  a horocycle is the intersection the hyperboloid with a plane whose normal vector is  $\lambda(x, y, \sqrt{x^2 + y^2})$ . Note that the family of horocycles centered at a given point can be parameterized by the magnitude of the translation from the plane through the origin. Through this lens a choice of ideal point corresponds to a choice of line through the origin in  $\mathbb{R}^2$  and the horocycle corresponds to a choice of point on this line (specifying the plane translation).

**Remark 3.2.** Isometries of hyperbolic space act on horocycles so choosing one horocycle for each marked point of  $S$  gives a well defined choice of horocycle at every developed lift by the action of the holonomy representation. See Figure 4

**Definition 3.3.** The *decorated Teichmüller space*  $\mathcal{T}'(S)$  associated to a surface  $S$  is the space of decorated hyperbolic structures on  $S$  up to diffeomorphisms homotopic to the identity fixing the marked points.

There is a natural map from decorated Teichmüller space to Teichmüller space ( $\mathcal{T}'(S) \rightarrow \mathcal{T}(S)$ ) given by forgetting the decoration. Each fiber of this map is  $\mathbb{R}_+^{c+p}$ .

### 3.1 Lambda Lengths

The decoration allows us to assign a value to each edge of triangulation independently from the other choices. This means when we perform a geometric flip only one of these values would change.

**Definition 3.4.** *The lambda length between two ideal points with chosen horocycles is  $e^{d/2}$  where  $d$  is the length of the geodesic between the horocycles. We take  $d$  to be negative if the two horocycles intersect.*

This definition is a little odd at first with two glaring questions: “why exponentiate?” and “why divide by 2?”. One small justification for exponentiating is that the lambda length is always positive. As we will see positivity will be an important theme going forward.

A stronger reason for these operations is that mutation and the relation to the cross ratio are much cleaner this way. To begin we will prove the “magic formula” for computing the length of the piece of a horocycle inside a triangle.

**Definition 3.5.** *The lambda angle at vertex  $v_1$  of a decorated ideal triangle is  $T_1^{23} = \frac{\lambda_{23}}{\lambda_{12}\lambda_{13}}$ .*

**Remark 3.6.** *It is clear that  $T_1^{32} = T_1^{23}$  as lambda lengths are symmetric.*

**Theorem 3.7.** *Given a decorated ideal triangle  $v_1, v_2, v_3$  the length of the horocycle centered at  $v_1$  between the geodesics connecting to  $v_2$  and  $v_3$  is  $T_1^{23}$*

*Proof.* This is easiest to see in the upper half plane where without loss of generality we can take  $(v_1, v_2, v_3)$  to be  $(\infty, 0, 1)$  (Figure 5a). Then the length we are computing is the length of the horizontal line at height

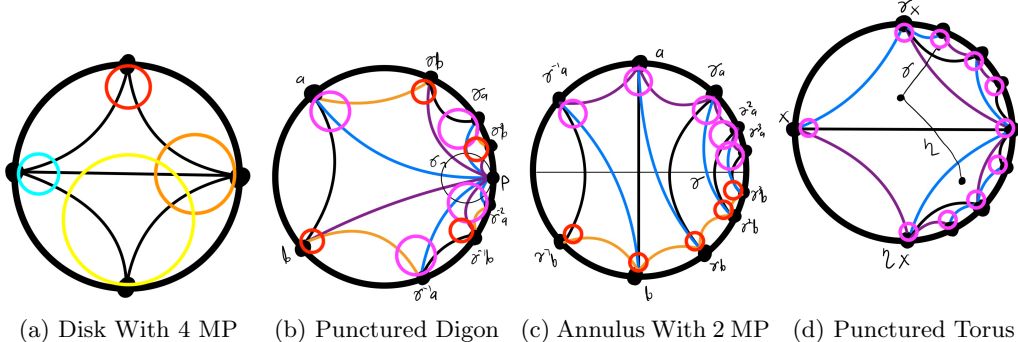


Figure 4: Decorated Developing Images Of Basic Examples

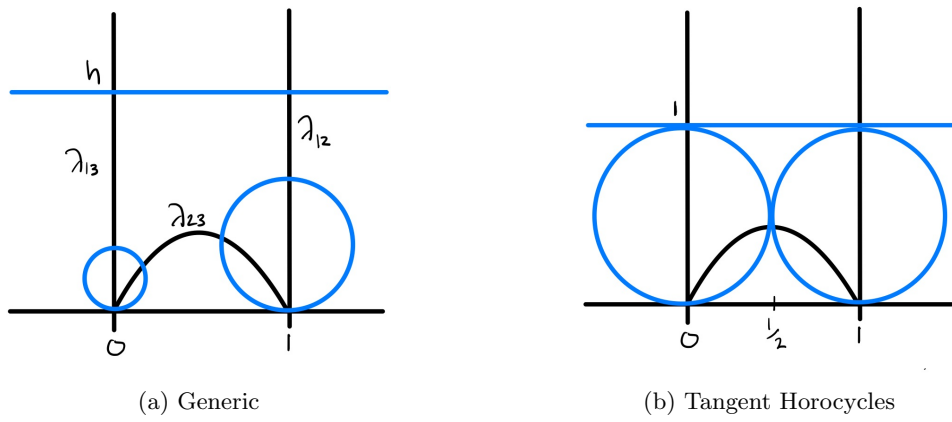


Figure 5: Ideal Decorated Triangle In Upper Half Plane Model

$h$  between 0 and 1. This is a simple computation

$$\int_{\gamma} \frac{ds}{y} = \int_0^1 dt \frac{1}{h} = \frac{1}{h}(1 - 0)$$

We then check how this length and the ratio of lambda lengths change as we change the size of the horocycles. We see that changing a horocycles at one end of the curve so the distance increases by  $\varepsilon$  changes the associated lambda length by  $e^{\varepsilon/2}$ .

$$\lambda'_{12} = e^{(d(v_1, v_2) + \varepsilon)/2} = \lambda_{12}e^{\varepsilon/2}$$

Changing the horocycle at  $v_2 = 0$  sends  $\lambda_{12} \mapsto \lambda_{12}e^{\varepsilon/2}$  and  $\lambda_{23} \mapsto \lambda_{23}e^{\varepsilon/2}$ . The  $e^{\varepsilon/2}$  cancels in  $T_1^{23}$  which matches the fact the horocycle length we are measuring hasn't changed. Similarly changing the horocycle at  $v_3 = 1$  fixes both sides.

It remains to see what happens when we move the horocycle at  $v_1 = \infty$  from  $h$  to  $he^\varepsilon$ . This is a shift by hyperbolic distance  $\varepsilon$  so  $\lambda_{12} \mapsto \lambda_{12}e^{\varepsilon/2}$  and  $\lambda_{13} \mapsto e^{\varepsilon/2}$ . Thus  $T_1^{23} = \frac{\lambda_{23}}{\lambda_{12}\lambda_{13}}$  is transformed by a factor of  $e^{-\varepsilon}$ . Similarly  $\frac{1}{h} \mapsto \frac{1}{he^\varepsilon} = \frac{1}{h}e^{-\varepsilon}$ .

Finally we check that these functions agree for some choice of horocycle. Take the horocycles that all meet at a single point (See Figure 5b). Then  $\lambda_{12} = \lambda_{23} = \lambda_{13} = 1$  and  $T_1^{23} = 1$ . In this configuration the horocycle centered at infinity is at height 1 and so the length of the horocyclic arc is also 1.  $\square$

**Remark 3.8.** *The  $\frac{1}{2}$  in the definition of lambda length was necessary for the ratio to transform correctly as the horocycle we were measuring varied.*

**Claim 3.9.** *The lengths of adjacent horocyclic arcs is additive. Symbolically  $T_1^{23} + T_1^{34} = T_1^{24}$*

We will use this additivity to derive a mutation rule for the geometric flip.

**Corollary 3.10.** *The lambda lengths corresponding to four decorated ideal points  $v_1, v_2, v_3, v_4$  satisfy the relation  $\lambda_{13}\lambda_{24} = \lambda_{12}\lambda_{34} + \lambda_{14}\lambda_{23}$*

*Proof.* We start with the additivity formula around  $v_1$ :

$$\begin{aligned} T_1^{24} &= T_1^{23} + T_1^{34} \\ \frac{\lambda_{24}}{\lambda_{12}\lambda_{14}} &= \frac{\lambda_{23}}{\lambda_{12}\lambda_{13}} + \frac{\lambda_{34}}{\lambda_{13}\lambda_{14}} \\ \lambda_{24}\lambda_{13} &= \lambda_{23}\lambda_{14} + \lambda_{34}\lambda_{12} \end{aligned}$$

$\square$

Explicitly this means that performing the geometric flip replacing the edge  $\gamma_{13}$  with  $\gamma_{24}$  correspond to replacing the coordinate  $\lambda_{13}$  with  $\lambda_{24} = \frac{\lambda_{12}\lambda_{34} + \lambda_{14}\lambda_{23}}{\lambda_{13}}$ . In the next lecture we will see this mutation relation will generalize to the  $A$  type cluster mutation rule.

**Claim 3.11.** *Given a triangulation the set of lambda lengths corresponding to the edges uniquely specifies the hyperbolic structure up the action of  $\text{PSL}(2, \mathbb{R})$ .*

*Proof.* We give an informal sketch here. Later we will discuss explicit formulas to reconstruct a decorated representation  $\rho: \pi_1(S) \rightarrow \text{PSL}(2, \mathbb{R})$ . After picking one triangle to send to  $(0, 1, \infty)$  the lambda lengths associated to these edges fix the horocycles centered on the vertices of the triangles. As we saw the lambda lengths in the next triangle specify the horocyclic length between the new geodesics which fixes the new ideal point and horocycle centered there.  $\square$

### 3.2 Relationship Between Lambda Lengths and Cross Ratios

Recall that the cross ratio was an invariant we associated to the diagonal edge of a square in the triangulation. If we label the vertices of the square  $v_1, \dots, v_4$  so the diagonal goes from  $v_1$  to  $v_3$  we have the following theorem:

**Theorem 3.12.** *The cross ratio  $X = \text{cr}(v_1, v_2, v_3, v_4)$  is equal to  $\frac{\lambda_{12}\lambda_{34}}{\lambda_{14}\lambda_{23}}$ .*

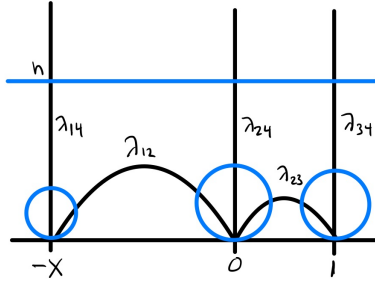


Figure 6: Decorated Ideal Square In The Upper Half Plane Model

*Proof.* Using  $\text{PSL}(2, \mathbb{R})$  we can send  $(v_1, v_2, v_3, v_4)$  to  $(-X, 0, 1, \infty)$ . Again we compute in the upper half space model (Figure 6). The horocycle centered at infinity is the horizontal line  $y = h$ . Then the length of this horocycle between  $-x$  and  $0$  is  $\frac{1}{h}X$ . From our magic formula (Theorem 3.7) we know this length is also  $\frac{1}{h}X = T_4^{12}$ . Similarly the length between  $0$  and  $1$  is  $\frac{1}{h} = T_4^{23}$ . Therefore

$$X = T_4^{12}(T_4^{23})^{-1} = \frac{\lambda_{12}}{\lambda_{14}\lambda_{24}} \frac{\lambda_{24}\lambda_{34}}{\lambda_{23}} = \frac{\lambda_{12}\lambda_{34}}{\lambda_{14}\lambda_{23}}$$

□

**Corollary 3.13.** *We can also write  $1 + X$  and  $1 + X^{-1}$  as ratios of lambda lengths. Explicitly:*

$$1 + X = \frac{\lambda_{13}\lambda_{24}}{\lambda_{14}\lambda_{23}} \quad 1 + X^{-1} = \frac{\lambda_{13}\lambda_{24}}{\lambda_{12}\lambda_{34}}$$

Using this relationship we can derive the mutation rule for cross ratios. We focus on a pentagon with initial triangulation  $\gamma_{13}$  and  $\gamma_{14}$ . Here we have two cross ratios which we can write in lambda lengths as

$$X_{13} = \frac{\lambda_{12}\lambda_{34}}{\lambda_{14}\lambda_{23}} \quad X_{14} = \frac{\lambda_{13}\lambda_{45}}{\lambda_{15}\lambda_{34}}$$

If we perform geometric exchange inside the square  $1234$  we replace  $\gamma_{13}$  with  $\gamma_{24}$ . Writing the new cross ratios here we obtain

$$X_{24} = \frac{\lambda_{14}\lambda_{23}}{\lambda_{12}\lambda_{34}} \quad X_{14} = \frac{\lambda_{12}\lambda_{45}}{\lambda_{15}\lambda_{24}}$$

By comparing with the old formulas we see the cross ratio at the mutated edge changed by inversion. However the neighboring cross ratio  $X_{14}$  changes by a factor of  $\frac{\lambda_{12}\lambda_{34}}{\lambda_{13}\lambda_{24}} = (1 + X_{13}^{-1})^{-1}$ .

We can perform a similar computation performing the exchange in the square  $1345$  replacing the arc  $\gamma_{14}$  with  $\gamma_{35}$ . The new cross ratios are

$$X_{13} = \frac{\lambda_{12}\lambda_{35}}{\lambda_{23}\lambda_{15}} \quad X_{35} = \frac{\lambda_{15}\lambda_{34}}{\lambda_{13}\lambda_{45}}$$

Now the adjacent cross ratio  $X_{13}$  changes by a factor of  $\frac{\lambda_{14}\lambda_{35}}{\lambda_{15}\lambda_{34}} = 1 + X_{14}$ .

Which rule to chose for the neighbor depends on if the neighbor comes before or after the exchanged arc in the clockwise orientation of the shared triangle. We will see in the next lecture that this generalizes into the  $X$  type cluster mutation rule.

## Part II

# Lecture II: Cluster Algebra Combinatorics

Last lecture we gave coordinates for decorated and undecorated Teichmüller space. In both cases the coordinates depended on some underlying combinatorial data, an ideal triangulation of the surface. Different triangulations are related by sequences of local operations, “geometric exchange”. In the decorated case we had a function associated to each edge, the lambda length and in the undecorated case we had a function for each interior arc. We remark that the interior arcs are the only edges that can exchanged. We now introduce a purely combinatorial generalization of the situation.

## 4 Definition of a Cluster Structure

### 4.1 Quiver Mutation

**Definition 4.1.** A *quiver*  $Q$  is a directed graph without self loops or two cycles. We divide the nodes into two sets which call **unfrozen** and **frozen**.

**Remark 4.2.** The unfrozen set is also called the **mutable** set.

**Remark 4.3.** In a triangulation of a surface each arc of the triangulation corresponds to a node of the quiver. The interior arcs are unfrozen or mutable as they can be exchanged. Correspondingly the boundary arcs are frozen nodes.

We now define a mutation rule for quivers.

**Definition 4.4.** We **mutate**  $Q$  at a node  $i$  to obtain a new quiver  $Q' = \mu_i(Q)$  in the following three step process:

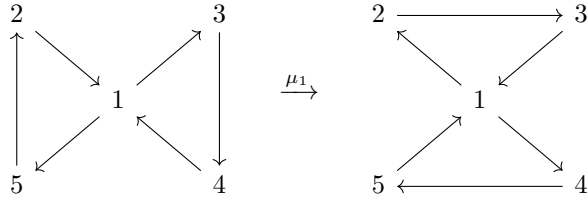
1. For each path of arrows through  $i$ ,  $j \rightarrow i \rightarrow k$  add an arrow  $j \rightarrow k$ .
2. Reverse all arrows incident to  $i$ .
3. Remove any two cycles formed by the previous steps.

**Claim 4.5.** Quiver mutation is an involution.

**Claim 4.6.** Quiver mutation at two nonadjacent nodes commute.

*Proof.* Since mutation at  $i$  only adds arrows between nodes adjacent to  $i$  it cannot change any paths of arrows through a nonadjacent node.  $\square$

**Example 4.7.** We mutate the following quiver at 1.



We now have enough to define a quiver associated to a triangulation of a surface so that geometric flips correspond to mutation of the quiver.

**Definition 4.8.** The quiver  $Q$  associated to a triangulation  $T$  has a node for each arc of  $T$ . For each triangle of  $T$  add a clockwise cycle of arrows between the nodes. If any two cycles appear cancel them. As described all interior arcs are unfrozen/mutable and all boundary arcs are frozen.

**Remark 4.9.** The quiver in Example 4.7 comes from the triangulation of a square.

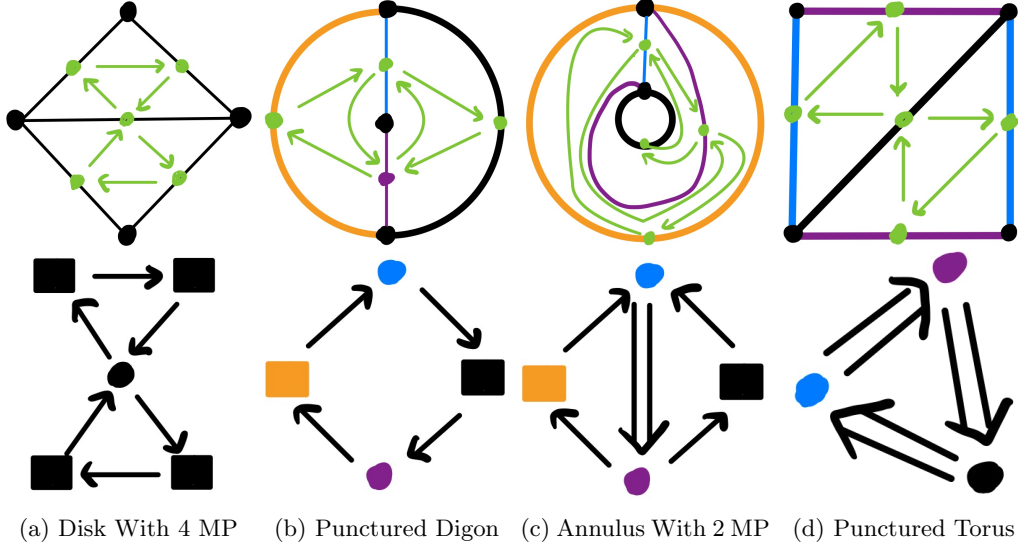


Figure 7: Quivers associated to basic surfaces

**Example 4.10.** In Figure 7 we see the quivers associated to our basic surfaces: disk with 4 marked points, punctured digon, annulus with two marked points, and punctured digon. We use square nodes to represent the frozen nodes which correspond to the boundary arcs. Note how in Figure 7b the arrows between the mutable node canceled while in Figure 7c the arrows added to form a double arrow.

## 4.2 A Coordinate Mutation

**Definition 4.11.** An *A coordinate* is a variable associated to a node of a quiver. To build an abstract cluster algebra, these coordinates are invertible elements of  $\mathbb{Z}(a_1^{\pm 1}, \dots, a_m^{\pm})$ . When building a cluster structure on a ring, the *A* coordinates are distinguished choices of elements of the ring.

**Example 4.12.** For the cluster structure on decorated Teichmüller space the *A* coordinates are the lambda lengths of arcs.

**Definition 4.13.** A *seed* of a cluster algebra is the pair of a quiver and choice of *A*-coordinate for each node. The set of *A* coordinates in a seed is called a *cluster*. The size of the unfrozen set is the *rank* of the seed and the corresponding cluster algebra.

We can extend quiver mutation to a mutation of seeds by defining the following mutation rule on *A* coordinates:

$$\mu_i(a_i) = \frac{1}{a_i} \left( \prod_{j \rightarrow i} a_j + \prod_{i \rightarrow k} a_k \right) \quad (4)$$

**Remark 4.14.** For the surface quiver this is exactly the relation of lambda lengths when performing geometric exchange.

**Example 4.15.** Consider the quiver  $1 \rightarrow 2$  with starting coordinates  $a_1, a_2$ .

Here the quiver mutation is very simple, we reverse the orientation of the unique arrow. If we mutate at the source we see the new variable will satisfy the relation  $a_n a_{n+2} = 1 + a_{n+1}$ . Note the empty product of arrows into the source is taken to be 1. Iterating this procedure we see:

$$\begin{aligned} a_3 &= \frac{1+a_2}{a_1} \\ a_4 &= \frac{1+a_3}{a_2} = \frac{1+\frac{1+a_2}{a_1}}{a_2} = \frac{1+a_1+a_2}{a_1 a_2} \\ a_5 &= \frac{1+a_4}{a_3} = \frac{1+\frac{1+a_1+a_2}{a_1 a_2}}{\frac{1+a_2}{a_1}} = \frac{a_1 a_2 + a_1 + 1 + a_2}{(1+a_2) a_2} = \frac{(1+a_1)(1+a_2)}{(1+a_2) a_2} = \frac{1+a_1}{a_2} \\ a_6 &= \frac{1+a_5}{a_4} = \frac{1+\frac{1+a_1}{a_2}}{\frac{1+a_1+a_2}{a_1 a_2}} = \frac{(1+a_1+a_2)a_1}{1+a_1+a_2} = a_1 \\ a_7 &= \frac{1+a_6}{a_5} = \frac{1+a_1}{\frac{1+a_1}{a_2}} = a_2 \end{aligned}$$

Remarkably this pattern repeats after finitely many steps  $a_{i+5} = a_i$ .

**Remark 4.16.** Every cluster variable is a Laurent polynomial in  $a_1, a_2$  with a unique denominator.

**Definition 4.17.** The **exchange graph** of a cluster algebra is a graph with vertices for each seed and an edge connecting two seeds related by a single mutation.

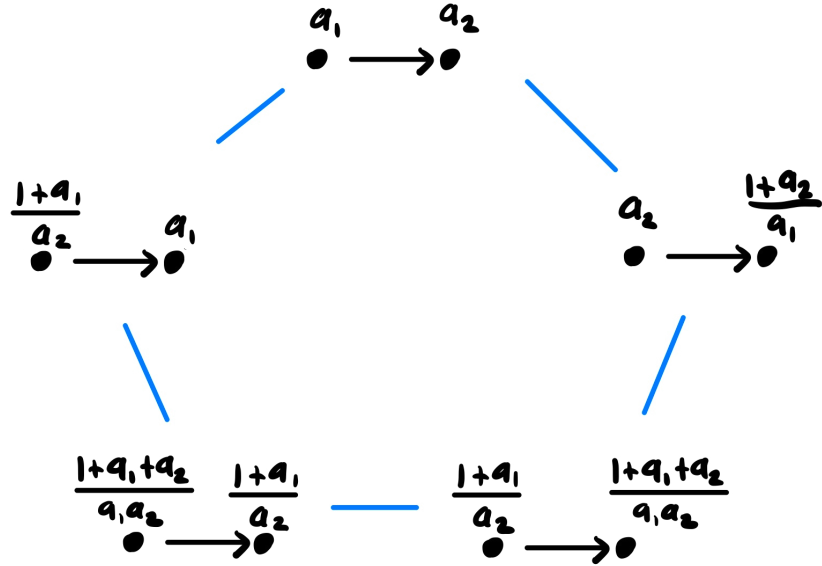


Figure 8: Exchange graph for the  $A_2$  cluster algebra

The exchange graph for the abstract  $A_2$  quiver is a pentagon (Figure 8). We now consider the cluster algebra structure for decorated hyperbolic structures on a pentagon. Here we start with a triangulation with edges  $e_{12}$  and  $e_{13}$ . The associated quiver has two mutable nodes with functions  $\lambda_{12}$  and  $\lambda_{13}$ . Performing all possible geometric exchanges/cluster mutations results in the same exchange graph as the abstract  $A_2$ . This is an example of the following theorem:

**Theorem 4.18.** The exchange graph of a cluster algebra is independent of the frozen nodes.

**Example 4.19.** We now consider the case of the annulus with 2 marked points.

In order to compute the geometric exchange we need to index arcs of the triangulation. Here every interior arc connects the two unique marked points on each boundary. The difference between arcs is the winding number  $i$ . Two arcs  $e_i$  and  $e_j$  are non-crossing if and only if  $|i - j| = 1$ . So there is a unique seed  $S_i$  with interior arcs  $e_i, e_{i+1}$ . Mutation at  $e_i$  results in  $e_{i+2}$  and so send  $S_i$  to  $S_{i+1}$ .

The quiver associated to each triangulation is the same. The mutable portion is a double edge connecting the two mutable nodes. Each boundary arc corresponds to a frozen node attached in a oriented cycle (Figure 7c). We observe that mutation returns this quiver to itself. We can start an equivalent abstract cluster algebra by starting with mutable  $A$  coordinate  $a_1, a_2$  and no frozen variables. Then we have  $a_{i+2}a_i = 1 + a_{i+1}^2$ .

$$\begin{aligned} a_3 &= \frac{1 + a_2^2}{a_1} \\ a_4 &= \frac{1 + a_3^2}{a_2} = \frac{a_1^2 + 1 + 2a_2^2 + a_2^4}{a_1^2 a_2} \\ a_5 &= \frac{1 + a_4^2}{a_3} = \frac{a_1^4 + 2a_1^2 + 1 + 2a_1^2 a_2^2 + 3a_2^2 + 3a_2^4 + a_2^6}{a_1^3 a_2^2} \end{aligned}$$

We see that the “minimal” degree of the polynomial in  $a_1, a_2$  changes with each mutation so this mutation never repeats. We can formalize this by **tropicalizing** the mutation rule. As the  $A$  coordinate mutation only involves addition, multiplication and division we can use any semiring for the coordinates. In this way we can track the minimal degree of a Laurent polynomial by taking “multiplication” to be sum of the degrees and “addition” to be take the minimal degree. We write the minimal degree as a vector  $(d_1, d_2)$  representing the minimal term  $a_1^{d_1} a_2^{d_2}$ . So the minimal degree of  $a_{i+2}$  is  $\min\{1, 2\text{mdeg}(a_{i+1}) - \text{mdeg}(a_i)\}$ :

$$\begin{aligned} a_1 &= (1, 0) \\ a_2 &= (0, 1) \\ a_3 &= \min\{(0, 0), 2(0, 1)\} - (1, 0) = (-1, 0) \\ a_4 &= \min\{(0, 0), 2(-1, 0)\} - (0, 1) = (-2, -1) \\ a_5 &= \min\{(0, 0), 2(-2, -1)\} - (-1, 0) = (-3, -2) \end{aligned}$$

**Remark 4.20.** Another reason that this cluster structure is infinite is because the surface has nontrivial mapping class group. This is because the mapping class group acts on triangulations of a surface while preserving “adjacency” of the triangles. Thus the mapping class group gives a subset of the symmetry of the exchange graph.

**Example 4.21.** We now look at the punctured digon.

Here the mapping class group is trivial so we expect a finite cluster algebra. In fact the quiver associated to the standard triangulation is two disconnected nodes (due to canceling the two cycle). The corresponding cluster complex is a square as the two mutations commute. However if we look at the surface, mutating either of the initial edges results in a self folded triangle. As such geometric exchange doesn’t make sense at the inner arc. However a slight modification to the combinatorics of triangulations of punctured surfaces can make these two methods agree. For more details see [FST08].

## 5 Laurent Phenomenon

**Theorem 5.1.** Every  $A$  coordinate in any seed obtained from an initial seed  $(Q, \mathbf{a})$  are Laurent polynomials in  $\mathbf{a}$ .

*Proof.* The proof is fairly technical, see [FWZ21b] □

**Conjecture 5.2.** *The coefficients of these polynomials are positive. In particular if the initial cluster variables are positive then all variables are positive.*

**Remark 5.3.** *This can be subtle as  $\frac{1+x^3}{1+x} = 1 - x + x^2$ .*

## 5.1 X Coordinate Mutation

We have seen how cluster  $A$  coordinates generalizes Lambda lengths on hyperbolic surfaces. We now define a set of coordinates and mutation rule that will correspond to the transformation of cross ratios.

**Definition 5.4.** *An  $X$  seed for a cluster algebra is the pair of a quiver  $Q$  and a choice of variables  $x_1$  to  $x_n$  for each mutable node of  $Q$ .*

We then describe a seed mutation at  $i$  by giving a mutation rule for  $X$  coordinates. To recall that each quiver corresponds to a skew symmetric matrix  $\varepsilon$  where  $\varepsilon_{ij}$  is the number of arrows from  $i$  to  $j$ . Then define:

$$\mu_i(x_k) = \begin{cases} \frac{1}{x_i} & i = k \\ x_k(1 + x_i)^{\varepsilon_{ik}} & \varepsilon_{ik} > 0 \\ x_k(1 + x_i^{-1})^{\varepsilon_{ik}} & \varepsilon_{ik} < 0 \end{cases} \quad (5)$$

**Remark 5.5.**  *$X$  mutation changes every coordinate incident to  $i$  not just  $i$ .*

**Remark 5.6.** *The  $X$  mutation doesn't use the frozen variables of the quiver. As such if we relate the  $A$  and  $X$  exchange complexes we see the exchange complex is independent of the frozen nodes.*

Last time we saw that the cross ratio of a square can be written as a ratio of lambda lengths  $\frac{\lambda_{12}\lambda_{34}}{\lambda_{14}\lambda_{34}}$ . We can define a map  $\rho$  from the  $X$  cluster algebra to the  $A$  cluster algebra generalizing this situation.

$$\rho(X_i) = \prod a_j^{\varepsilon_{ij}} = \frac{\prod a_k}{\prod_{j \rightarrow i} a_j} \quad (6)$$

**Theorem 5.7.** *Let  $(Q, \mathbf{a})$  and  $(Q, \mathbf{x})$  be  $A$  and  $X$  seeds associated to the same quiver  $Q$ . After performing mutation at  $i$  to obtain  $(Q', \mathbf{a}')$  and  $(Q', \mathbf{x}')$  the two seeds are still related by  $\rho$ .*

*Proof.* We observe that under  $\rho$ ,  $1 + x_i$  is also mapped

$$\rho(1 + x_i) = 1 + \rho(x_k) = 1 + \frac{\prod a_k}{\prod_{j \rightarrow i} a_j} = \frac{\prod a_k + \prod_{j \rightarrow i} a_j}{\prod_{j \rightarrow i} a_j} = \frac{a_i a'_i}{\prod_{j \rightarrow i} a_j}$$

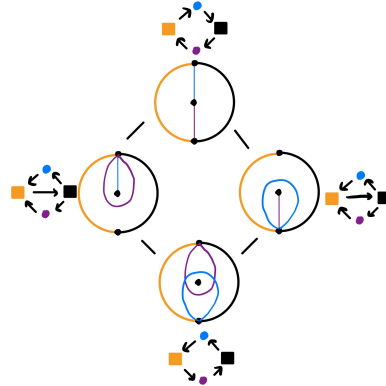


Figure 9: Cluster complex for punctured digon

Similarly  $\rho(1 + x_i^{-1}) = \frac{a_i a'_i}{\prod_{i \rightarrow k} a_k}$ . It is then a small calculation to compute  $\rho(x'_k)$  when  $i \xrightarrow{w} k$  ( $\varepsilon_{ik} = w$  for positive  $w$ ).

$$\rho(x'_k) = \frac{\prod_{k \rightarrow s} a_s}{\prod_{t \rightarrow k} a_t} \left( \frac{a_i a'_i}{\prod_{j \rightarrow i} a_j} \right)^w$$

As  $i \xrightarrow{w} k$  the  $a_i^w$  in the numerator will cancel with corresponding denominator term in the first fraction. In  $Q'$  the arrows incident to  $i$  are reversed so the  $a_i'^w$  should be in the numerator. Similarly for any path  $j \rightarrow i \rightarrow k$  we added  $j \rightarrow k$  and so  $a_j$  should appear in the denominator.

A similar computation shows that the  $x$  coordinates along “in edges” also transform in the same way.  $\square$

**Remark 5.8.** *It is useful to write  $X$  coordinates using their image under  $\rho$ . However the ratio of  $A$  coordinates might not uniquely identify  $X$  coordinates. This can be fixed by adding more frozen  $A$  coordinates. For example consider the quiver  $1 \rightarrow 2 \leftarrow 3$ . Here  $\rho(x_1) = a_2$  and  $\rho(x_3) = a_2$ . However adding different frozen variables  $f_1$  and  $f_3$  attached in to 1 and 3 respectively fixes the problem.*

## 6 Finite Type Classification

We observed in Example 4.19 that the cluster structure associated to a double edge is infinite. Clearly any cluster algebra with a seed containing a double edge is also infinite. Surprisingly this is the only obstruction to finiteness.

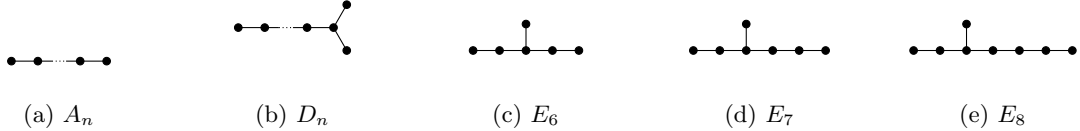


Figure 10: Simply Laced Finite Dynkin Diagrams

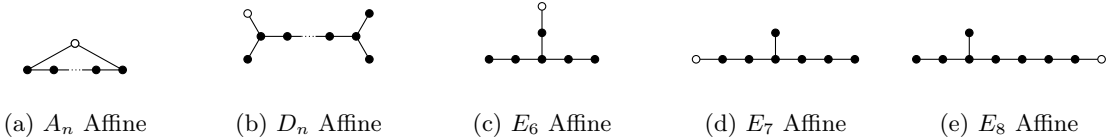


Figure 11: Simply Laced Affine Dynkin Diagrams

**Theorem 6.1.** *If every quiver mutation equivalent to  $Q$  has only single weight edges then the exchange complex associated to  $Q$  is finite. Moreover such a quiver is mutation equivalent to an orientation of a simply laced finite type Dynkin diagram (Figure 10).*

*Proof.* We give a sketch of the proof. For full detail see [FWZ21c].

First we claim that any quiver mutation equivalent to an orientation of an acyclic graph is mutation equivalent to all orientations of the graph. This can be checked inductively after noting that mutation at a source or sink preserves the underlying graph. Then one can show that if  $Q$  is mutation equivalent to an orientation of affine Dynkin diagram (Figure 11) then  $Q$  is mutation equivalent to a quiver with a double edge. There is a small exception, because the affine  $A_n$  diagram is a cycle. It turns out that there is an invariant of

the mutation class of a cycle which is the number of clockwise/counterclockwise arrows. A fully oriented cycle is actually finite as it can be obtained a triangulation of a punctured  $n$ -gon. However a cycle with  $p$  clockwise and  $q$  counterclockwise arrows is obtained by triangulating an annulus with  $p$  marked points on one boundary and  $q$  on the other. Similarly the affine  $D_n$  diagram can be obtained by triangulation an  $n$ -gon with two punctures. Both of these surfaces have infinite mapping class group and thus are infinite. It remains to explicitly verify that the affine  $E_6$ ,  $E_7$  and  $E_8$  are mutation equivalent to a quiver with double edge.

It then suffices to show the quivers mutation equivalent to finite Dynkin diagrams are finite. There are two infinite families of finite Dynkin diagrams  $A_n$  and  $D_n$ . We can observe that these correspond to triangulations of  $n+3$ -gons ( $A_n$ ) and punctured  $n$ -gons ( $D_n$ ). As the mapping class group of both these surfaces are finite we observe there are finitely many possible arcs and thus finitely many possible triangulations. The final cases  $E_6, E_7, E_8$  can be computed explicitly. Here a computer is useful as  $E_8$  has 25080 seeds. In Figure 12 we see the full exchange graph for  $E_6, E_7$  and  $E_8$

□

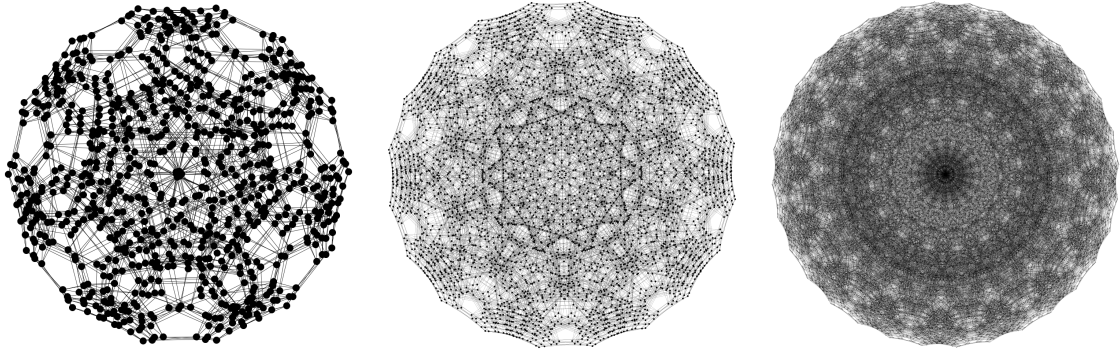


Figure 12: Exchange Graphs For  $E_6, E_7, E_8$

**Theorem 6.2.** *In every finite cluster algebra starting from a seed  $(Q, \mathbf{a})$  the denominator of each Laurent polynomial uniquely identifies the polynomial. In fact if  $Q$  is an orientation of a finite Dynkin diagram such that every node is a source or a sink we get an easy injective map from cluster variables to roots of the corresponding root system. If we label the roots  $\alpha_1, \dots, \alpha_n$  and the  $A$  coordinates at the corresponding locations on the Dynkin diagram  $a_1, \dots, a_n$  the map is*

$$\frac{p_{\mathbf{d}}(\mathbf{a})}{a_1^{d_1} \dots a_n^{d_n}} \mapsto \sum d_i \alpha_i$$

*Proof.* The proof is fairly technical but amounts to translating the “tropical mutation rule for denominator vectors” into an operation of root systems. See [FZ03] for full detail. The image of this map is the positive roots plus negative the simple roots (for the starting cluster). □

**Corollary 6.3.** *A consequence of the proof of the previous theorem is that every  $A$  coordinate appears on a quiver isomorphic to  $Q$ .*

**Claim 6.4.** *For any quiver  $Q$  which is a orientation of a acyclic graph such that every node is a source or a sink the mutation sequence mutate at every source then mutate at every sink returns to an isomorphic quiver.*

We note this operation is well defined as sources/sinks cannot be adjacent and mutation at nonadjacent nodes commutes. We call this the **sources-sinks mutation sequence**.

In the cluster algebras of finite type the order of the sources sinks mutation is finite and is related to the Coxeter number  $h$  of the associated Dynkin diagram.

**Claim 6.5.** *The order of the sources sink mutation for a finite type cluster algebra is  $\frac{h+1}{2}$ .*

## 6.1 Cluster Subalgebras

**Definition 6.6.** *A **cluster subalgebra** of cluster algebra is obtained by “freezing” some of the mutable nodes in a seed  $(Q, \mathbf{a})$ . In other words the subcluster algebra structure is obtained by choosing a set of  $A$  coordinates that will appear in every seed of the subalgebra.*

**Definition 6.7.** *We can upgrade the exchange graph to the **exchange complex** which has a  $k$  cell for each rank  $k$  subalgebra. The boundary of each cell is all corank 1 subalgebras.*

We note that a rank 0 subalgebra consists of a single seed as every node of the quiver is frozen. Similarly a rank 1 subalgebra is an edge corresponding to a single mutation as there is one mutable node and the boundary is the two seeds obtained by mutating at that node.

**Theorem 6.8.** *The type of every subalgebra of a cluster algebra of finite type is obtained by removing nodes of the corresponding Dynkin diagram.*

*Proof.* From Corollary 6.3 we know every  $A$  coordinate appears on a quiver corresponding to a sources-sinks orientation of a Dynkin diagram. Thus every codimension 1 subalgebra has type given by removing one node from the Dynkin diagram. Inductively this is true for all subalgebras.  $\square$

**Example 6.9.** *The codimension 1 subalgebras of an  $A_3$  cluster algebra are of type  $A_2$  or  $A_1 \times A_1$ . In fact there are twice as many  $A_2$  subalgebras as  $A_1 \times A_1$ . For an exact count we know that the sources-sinks mutation has order 3 and so the  $A_3$  cluster algebra has 6  $A_2$  subalgebras and 3,  $A_1 \times A_1$  subalgebras (Figure 13)*

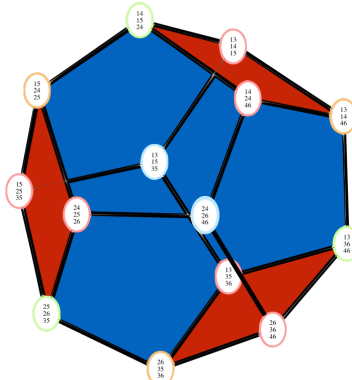


Figure 13: Exchange Complex of type  $A_3$

# Part III

## Lecture $\gamma$ : Grassmannians

### 7 Grassmannian Basics

In this lecture we will define and explore the cluster structure on the Grassmannian. What follows is modeled on [FWZ21a] and [Sco06]. First we need to recall what the Grassmannian is.

**Definition 7.1.** *The Grassmannian  $Gr(k, n)$  is the set of  $k$  dimensional linear subspaces of  $\mathbb{R}^n$ .*

In algebraic geometry one often uses the notation  $Gr(p, q)$  to mean  $Gr(p, p + q)$  in our notation. People often consider the complex Grassmannian. Most of what follows will work over  $\mathbb{C}$  as well, except for the discussion of positivity.

A natural question is to give coordinates to this space. Our first attempt is to represent each  $k$  dimensional subspace by a set of  $k$  vectors in  $\mathbb{R}^n$ , i.e. an  $k \times n$  matrix. However the same point is represented by many different matrices/ has many different bases. The solution to this is the Plücker embedding.

**Definition 7.2.** *For each  $I \subseteq \{1, \dots, n\}$  of size  $k$  the Plücker coordinate  $p_I : Gr(k, n) \rightarrow \mathbb{R}$  is given by taking the determinant of the submatrix with columns  $i \in I$  of a matrix representing a point in  $Gr(k, n)$ . The Plücker embedding is the combined map  $Gr(k, n) \rightarrow \mathbb{P}^N \mathbb{R}$  for  $N = \binom{n}{k} - 1$  given by all possible Plücker coordinates.*

The Plücker embedding is well defined as the representative matrix is well defined up to left multiplication by  $m \in GL(k)$ . This simultaneously changes all Plücker coordinates by  $\det(m)$  and thus gives a well defined point in projective space.

**Remark 7.3.** *We extend the definition of Plücker coordinates to ordered tuples by setting*

$$p_{i_1, \dots, i_k} = (-1)^\sigma p_{i_{\sigma(1)}, \dots, i_{\sigma(k)}}$$

where  $(-1)^\sigma$  is the sign of the permutation  $\sigma$ . Similarly if any index repeats we take the corresponding Plücker coordinate to be zero. This follows naturally from viewing the Plücker coordinate as a determinant.

The set of Plücker coordinates is not algebraically independent. In fact for each sequence  $i_1 < \dots < i_{k-1}$  and  $j_1 < \dots < j_{k+1}$  there is a relation

$$0 = \sum_{\ell=1}^{k+1} (-1)^\ell p_{i_1, \dots, i_{k-1}, j_\ell} p_{j_1, \dots, \hat{j}_\ell, \dots, j_{k+1}}$$

When the two chosen sets share  $k - 2$  indices the relation simplifies dramatically. If  $I$  is the set of common indices and  $i < j < k < \ell$  is a disjoint choice of indices we have:

$$0 = p_{ijI} p_{k\ell I} - p_{ikI} p_{j\ell I} + p_{i\ell I} p_{jkI} \tag{7}$$

$$p_{ikI} p_{j\ell I} = p_{ijI} p_{k\ell I} + p_{i\ell I} p_{jkI} \tag{8}$$

This relation has the form of a cluster  $A$  mutation! In fact when  $k = 2$  the set  $I$  is empty and the relation is exactly the same as the relation of the lambda lengths in a square cyclicly labeled  $i, j, k, \ell$ .

$$p_{ik} p_{j\ell} = p_{ij} p_{k\ell} + p_{i\ell} p_{jk}$$

These relations give the Grassmannian the structure of a projective variety. In other words the image of the Plücker embedding is exactly the variety cut out by the Plücker relations. So studying the Grassmannian is

related to studying its coordinate ring  $\mathbb{R}[\text{Gr}(k, n)]$ , the ring of polynomials in Plücker coordinates up to the Plücker relations. In what follows we actually consider the affine cone over the Grassmannian  $\widehat{\text{Gr}(k, n)}$  and the corresponding coordinate ring  $\mathbb{R}[\widehat{\text{Gr}(k, n)}]$ . This is mostly a technicality and so in the remainder of the lecture we will write  $\text{Gr}(k, n)$  for the affine cone.

## 8 Cluster Structure on the Grassmannian

To construct a cluster structure on the (coordinate ring) of the Grassmannian we need to describe a starting seed, quiver and set of functions so that

1. Every element of the coordinate ring is in the algebra spanned by the  $A$  coordinates.
2. Every  $A$  coordinate generated by mutation is in the coordinate ring.

The first condition is satisfiable by choosing the initial functions to be a generating set for the ring. We also want the set to be algebraically independent so that all relations come from the cluster structure. The second condition is harder to guarantee as the mutation rule involves division, and so the new  $A$  coordinates might not be regular. Fortunately we have a lemma which restricts our testing to a single seed and its neighbors rather than the whole cluster structure.

**Lemma 8.1** (Starfish Lemma). *Let  $R$  be a finitely generated  $\mathbb{C}$  algebra with unique factorization. Let  $F$  be the corresponding fraction field. If  $(Q, \mathbf{a})$  is the seed a cluster algebra such that*

1. *Every coordinate of the seed is in  $R$ .*
2. *The elements of  $\mathbf{a}$  are pairwise coprime.*
3. *Every mutation at  $a_k$  resulting in a new coordinate  $a'_k$  also in  $R$  such that  $a_k$  and  $a'_k$  are coprime.*

*then the cluster algebra generated by the seed is contained in  $R$ .*

*Proof.* For full details of the proof see [FWZ21a]. Informally it suffices to check regularity outside a variety of codimension 2 (Hartog's continuation principle). We define  $Y$  the variety of points where two variables vanish between our initial seed and its neighbors.

$$Y = \bigcup_{1 \leq i \leq j \leq n} \{a_i = a_j = 0\} \cup \bigcup_{1 \leq k \leq n} \{a_k = a'_k = 0\}$$

The variables being coprime ensures that at least two equations are needed to define any of these subsets. Furthermore on the complement only a single variable in the original seed  $a_k$  can be zero. Then either  $a_k$  or  $a'_k$  is nonzero. As any cluster coordinate is a Laurent polynomial either in the original seed or this neighbor it must be regular.  $\square$

In  $\text{Gr}(2, n)$  we have a simple construction for a seed given by a triangulation of an  $n$ -gon. Each edge of the triangulation connecting boundary points  $i$  and  $j$  corresponds to the Plücker coordinate  $p_{ij}$ . This set of coordinates is independent as no edge “crosses” and every Plücker relation requires a crossing edge. Moreover the relation given by a geometric flip corresponds exactly to a Plücker relation and so mutation in every direction satisfies the starfish lemma. It is difficult to check any seed generates the ring directly, but as every Plücker coordinate is realized as the edge of some triangulation we know we get all the generators. Thus we would like a construction of a similar “maximal non crossing” set for  $\text{Gr}(k, n)$  generalizing  $\text{Gr}(2, n)$ . Recall that for each  $1 \leq i \leq n$  we have an inclusion  $\text{Gr}(k, n) \hookrightarrow \text{Gr}(k+1, n+1)$  given by  $p_I \mapsto p_{i \cup I}$ . Under  $\rho_5$  two non crossing coordinates  $p_{12}$  and  $p_{34}$  map to  $p_{125}$  and  $p_{345}$ . This motivates the following definition.

**Definition 8.2.** Two subsets  $I$  and  $J$  of  $\{1, \dots, n\}$  of size  $k$  are **non crossing** or **compatible** if every arc between points  $I \setminus J$  doesn't cross any arcs between points in  $J \setminus I$ .

**Example 8.3.** The sets  $\{1, 2, 3\}$ ,  $\{2, 3, 5\}$  and  $\{2, 4, 5\}$  are pairwise compatible.

**Example 8.4.** The sets  $\{1, 2, 5\}$  and  $\{3, 4, 6\}$  are crossing. So is  $\{1, 3, 5\}$  and  $\{2, 4, 5\}$ .

**Lemma 8.5.** A set of  $k$  adjacent indices under the cyclic order is compatible with any other  $k$  subset of  $\{1, \dots, n\}$ .

*Proof.* Without loss of generality consider the set  $1, \dots, k$ . Then the only remaining indices in  $J \setminus I$  are between  $k+1$  and  $n$  which don't cross  $1k$ .  $\square$

For this reason the adjacent subsets will appear in every seed in  $\text{Gr}(k, n)$  and will be our frozen nodes.

**Claim 8.6.** The maximum size of a set of pairwise non crossing coordinates in  $\text{Gr}(k, n)$  is  $k(n-k)+1$ .

*Proof.* This is technical so we omit it here (see [LZ98])  $\square$

This result gives a recipe to construct maximal families of non crossing subsets in  $\text{Gr}(k, n+1)$  from such a family in  $\text{Gr}(k, n)$ . We start with  $\text{Gr}(k, n+1)$ . There are  $k$  adjacent subsets in  $\text{Gr}(k, n+1)$  that contain  $n+1$ . These sets are non crossing with every other set, so can be added to a family of size  $k(n-k)+1$  to obtain  $k(n+1-k)+1$  subsets which is the maximal number.

Furthermore we note that in  $\text{Gr}(k, k+1)$  the maximum size is  $k+1$  which is the number of adjacent subsets. We now need to describe how to build a seed inductively from this construction. In  $\text{Gr}(k, k+1)$  connect the adjacent set starting with  $i$  to  $i+1$  in an oriented cycle. Then to get a seed in  $\text{Gr}(k, n+1)$  from one in  $\text{Gr}(k, n)$  we add the  $k$  new frozen vertices (connected  $f_i$  to  $f_{i+1}$ ). These attach to the old frozen vertices which are no longer adjacent in oriented 3 cycles. See example in Figure 14.

We remark that the nodes of this quiver can be arranged in a  $k \times n-k$  grid (with the exception of one frozen

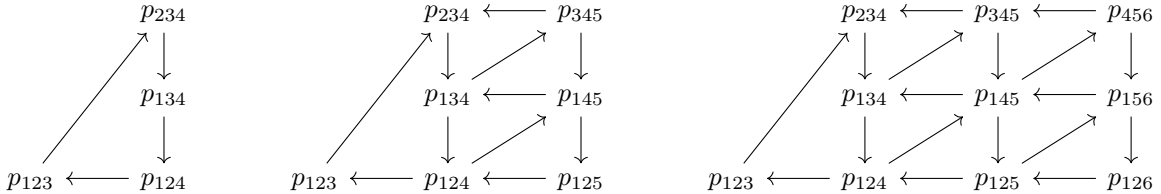


Figure 14: Constructing Seeds in  $\text{Gr}(3, 5)$  and  $\text{Gr}(3, 6)$  from  $\text{Gr}(3, 4)$

node). This is our candidate seed for  $\text{Gr}(k, n)$ . We must show that these coordinates generate the ring and satisfy the starfish lemma.

**Remark 8.7.** Any mutation of this quiver at a “2 in 2 out” location produces a new Plücker coordinate.

*Proof.* If we inspect the construction it is true for the initial quiver. A full proof requires the notion of an alternating strand diagram [Sco06].  $\square$

**Claim 8.8.** By starting with the top right node and mutating in successive diagonals we obtain a quiver that is a grid with no diagonals. There is a minor technicality that mutating diagonal  $i$  removes edges along diagonal  $i+1$  and adds the diagonals behind at diagonal  $i-1$ . This is fixed by mutating recursively at  $i-2$  to “push these edges off the quiver.”

The quiver in the previous claim is good because every mutable node is “2 in 2 out” and so checking the starfish condition is easy.

**Lemma 8.9.** Every Plücker coordinate appears in some seed connected to our initial seed.

*Proof.* This is true inductively using our embedding of  $\text{Gr}(k, n)$  in  $\text{Gr}(k, n+1)$  and  $\text{Gr}(k+1, n+1)$ .  $\square$

## 9 Analysis of Cluster Structure of Grassmannian

### 9.1 Positivity

One consequence of the cluster structure is identifying a minimal test for positivity.

**Definition 9.1.** *The **positive** Grassmannian is the subset of  $\text{Gr}(k, n)$  such that every Plücker coordinates are nonnegative.*

**Remark 9.2.** *This subset has many applications to theoretical physics including the calculation of scattering amplitudes in Yang Mills Theory.*

Each seed gives a minimal set of checks for every Plücker coordinates to be positive. This follows directly from the (positive) Laurent Phenomena. As  $k(n-k)+1$  is asymptotically smaller than  $\binom{n}{k}$  this is a significant computational improvement.

### 9.2 Non Plücker Coordinates

We can also use our general cluster theory to analyze the cluster structure of Grassmannians. Recall that the only finite cluster algebras are those mutation equivalent to an  $A_n$ ,  $D_n$  or  $E_6, E_7, E_8$  Dynkin diagram.

**Theorem 9.3.** *The cluster structure on  $\text{Gr}(k, n)$  is finite iff  $(k-2)(n-k-2) < 4$ . When  $k \leq \frac{n}{2}$  these  $\text{Gr}(2, n)$ ,  $\text{Gr}(3, 6)$ ,  $\text{Gr}(3, 7)$ , and  $\text{Gr}(3, 8)$ .*

*Proof.* We can check that the seed we construct for  $\text{Gr}(2, n)$  is type  $A_{n-3}$ . Alternately  $\text{Gr}(2, n)$  corresponds to triangulations of an  $n$ -gon which is finite. The remaining are of type  $D_4, E_6$  and  $E_8$  respectively. We check that if  $(k-2)(n-k-2) \geq 4$  then the cluster algebra is mutation equivalent to a quiver containing an  $(k-1)(n-k-1)$  grid. Such a grid contains an affine Dynkin diagram. In particular in either a  $3 \times 3$  grid ( $\text{Gr}(4, 8)$ ) or a  $2 \times 5$  grid ( $\text{Gr}(3, 9)$ ) we find a  $D_6$  affine.  $\square$

We also saw that in the finite cases the number of mutable cluster variables is the number of almost positive roots  $n(\frac{h}{2} + 1)$  where  $h$  is the Coxeter number of the rank  $n$  diagram. Thus the total number of cluster variable in  $\text{Gr}(k, n)$  adds  $n$  frozen variables. For  $\text{Gr}(2, n)$  which is type  $A_{n-3}$  this is

$$(n-3)\left(\frac{n-3}{2} + 1\right) + n = \frac{n(n-3)}{2} + n = \frac{n^2 - 3n + 2n}{2} = \frac{n(n-1)}{2} = \binom{n}{2}$$

Thus every cluster variable is a Plücker coordinate. However for  $\text{Gr}(3, 6)$  which is type  $D_4$  the Coxeter number is  $2 \cdot 4 - 2 = 6$ . So the number of A coordinates is  $4\left(\frac{6}{2} + 1\right) + 6 = 22$  and  $\binom{6}{3} = 20$ . This leaves 2 “exotic” coordinates. In Scott he calls them  $X$  and  $Y$ . We can find Laurent expressions for one them using cluster mutation from our constructed diagram.

$$\begin{aligned} Y \cdot p_{145} &= p_{125}p_{134}p_{456} + p_{156}p_{124}p_{345} \\ &= (p_{124}p_{135} - p_{123}p_{145})p_{456} + p_{124}(p_{135}p_{456} - p_{145}p_{356}) \\ &= p_{145}(-p_{123}p_{456} + p_{124}p_{356}) \end{aligned}$$

We can also write  $Y$  as  $\det(v_1 \times v_6, v_2 \times v_3, v_4 \times v_5)$ . The other coordinate is  $X = \det(v_1 \times v_2, v_3 \times v_4, v_5 \times v_6)$ . In this way the cluster structure reveals an additional symmetry of  $\text{Gr}(3, 6)$  called the “parity transformation”.

Similarly  $\text{Gr}(3, 7)$  is type  $E_6$  which has Coxeter number 12. Thus it has  $6 \cdot 7 + 7 = 49$  A coordinates which is 14 more than the  $\binom{7}{3} = 35$  expected. These “exotic” A coordinates corresponding to the 7 possible inclusions of  $\text{Gr}(3, 6)$  in  $\text{Gr}(3, 7)$ .

Finally  $\text{Gr}(3, 8)$  is type  $E_8$  and has Coxeter number 30. There are  $8 \cdot 16 + 8 = 136$  A coordinates compared to  $\binom{8}{3} = 56$  Plücker coordinates. There are  $\binom{8}{2} = 28$  embeddings of  $\text{Gr}(3, 6)$  in  $\text{Gr}(3, 8)$  corresponding to 56 images of  $X$  and  $Y$ . This leaves 24 coordinates. They are degree 3 polynomials in Plücker variables and come in two orbits under the standard dihedral action. For further details see Scott.

### 9.3 Finite Mutation Type

The two Grassmannians on the border between finite and infinite have a special classification. Both  $\mathrm{Gr}(3, 9)$  and  $\mathrm{Gr}(4, 8)$  are **finite mutation type**. In other words they have finitely many quivers despite having infinitely many cluster variables. This makes them more tractable than the higher Grassmannians but still difficult. See [KG21] for computations of the symmetry groups of “doubly extended cluster algebras” of which  $\mathrm{Gr}(4, 8)$  and  $\mathrm{Gr}(3, 9)$  are two important examples.

## Part IV

# Lecture iv: Cluster Structure on Double Bruhat Cell

In this lecture we explore the cluster structure on a new geometric object. When  $G$  is a simply connected semisimple Lie Group we have an explicit cluster structure for each **double Bruhat cell**. This explicit recipe gives us a concrete understanding of the ring of regular functions. What follows is loosely based on [BFZ05].

## 10 Notation and Definitions

First we fix our notation. We let  $G$  be a semisimple Lie Group. The key example is type  $A_{n-1}$  or  $G = \mathrm{SL}(n, \mathbb{C})$ . What follows generalizes nicely to the other simply laced Lie Groups ( $D_n, E_6, E_7, E_8$ ) although the computations are more complicated. The non simply laced examples ( $B_n = \mathrm{SO}(n, n+1)$ ,  $C_n = \mathrm{SP}(2n, \mathbb{R})$ ) require a slight generalization of cluster algebras but otherwise look more like the  $\mathrm{SL}(n, \mathbb{C})$  case.

**Definition 10.1.** *We say that an algebraic subgroup  $P$  is **parabolic** if  $G/P$  is a complete variety. Then a Borel subgroup is a parabolic subgroup with the “largest” possible quotient  $G/B$ . In  $\mathrm{SL}(n, \mathbb{C})$  we take  $B = B^+$  to be the subgroup of upper triangular matrices (with diagonal arbitrary and nonzero). Each Borel subgroup is paired with an **opposite Borel**. In  $\mathrm{SL}(n, \mathbb{C})$  this is the group of lower triangular matrices and we denote it  $B^-$ .*

The varieties  $G/P$  for  $P$  parabolic are called **flag varieties** and are of special interest when studying representations of surface groups and symmetric spaces. When  $P = B$  is Borel this variety is the **full flag variety**.

**Definition 10.2.** *The **maximal torus** is the intersection of  $B^+$  and  $B^-$ . In our  $\mathrm{SL}(n, \mathbb{C})$  setup this is the set of diagonal matrices and denoted  $H$ .*

**Definition 10.3.** *The **unipotent radical** of a parabolic subgroup  $P$  is denoted  $U$ . In our running example the unipotent radical of  $B^+$  is upper triangular matrices with all diagonal elements 1. Similarly  $U^-$  is the group of lower triangular matrices with diagonal 1. We have that  $P = H \rtimes U$ .*

A **decorated flag variety** is the quotient space  $G/U$  for some  $U$ .

### 10.1 Roots and Weights

Recall that each semisimple Lie group  $G$  has an associated Lie algebra  $\mathfrak{g}$ . The Lie algebra associated to the maximal torus  $H$  is  $\mathfrak{h}$ . This has a root system and Weyl group  $W$ .

**Definition 10.4.** *Abstractly **root** is a function  $\mathfrak{h} \rightarrow \mathbb{R}$  such that there is an  $X \neq 0$  in the Lie algebra so  $[H, X] = \alpha(H)X$ .*

**Definition 10.5.** *A **coroot** is a dual element to a root  $\alpha$  written  $\alpha^\vee$ . It is defined by how it pairs with  $X$  using the Killing form on the Lie algebra.*

**Definition 10.6.** *The **fundamental weights** is again a function  $\mathfrak{h} \rightarrow \mathbb{R}$  dual to a coroot under the “standard” dual basis construction. In otherwords the weight  $w_j$  dual to a coroot  $\alpha_i^\vee$  is one such that  $\alpha_i^\vee(w_j) = \delta_{ij}$ .*

We can extend the action of weight to  $H$  via  $w_j(e^h) = e^{w_j(h)}$ . This then extends to the entire group as generic elements can be decomposed  $B^- H B^+$ .

The correct choices of roots make the actual computations much simpler. For example in  $\mathrm{SL}(n, \mathbb{C})$  the root system (and associated Dynkin diagram) is of type  $A_{n-1}$ . For our choice of simple root spaces we take the upper off diagonal. We write  $e_i(a)$  for the matrix with  $a$  in position  $(i, i+1)$  and all other entries 0. In this way the root space associated to root  $\alpha_i$  is  $\{e_i(a) | a \in \mathbb{C}\}$ . The negative simple root spaces are  $f_i = e_i^T$ . We write  $X_i(a) = \exp(e_i(a)) = I + e(i)(a)$  for the corresponding element of the Lie Group  $\mathrm{SL}(n, \mathbb{C})$ . Similarly  $Y_i = \exp(f_i(a))$ . Note that under this convention the positive unipotent radical is generated by  $\{X_i\}$  and the negative unipotent radical is generated by  $\{Y_i\}$ .

In this scenario the fundamental weights  $w_i = \alpha_1 + \dots + \alpha_i$ . As a function on  $\mathrm{SL}(n, \mathbb{C})$  this is the determinant of the first  $i$  rows and columns.

## 10.2 Weyl Group

**Definition 10.7.** *The **Weyl Group** of a root system is the subgroup of the isometries of the root system generated. Concretely the Weyl group is given by an order two generator  $s_i$  for each node of the corresponding Dynkin diagram. The generators satisfy braid relations depending on the connection in the diagram. If  $i$  and  $j$  are not adjacent then  $s_i s_j = s_j s_i$ . However when  $i$  is adjacent to  $j$  we have  $s_i s_j s_i = s_j s_i s_j$ .*

The Weyl group can also be realized “in” the Lie group as  $\mathrm{Norm}_G(H)/H$ . In particular we can define lifts  $\bar{s}_i$  using our notation so far. We set  $\bar{s}_i = X_i(-1)Y_i(1)X_i(-1)$ . For example in  $\mathrm{SL}(n, \mathbb{C})$  we can compute

$$\bar{s}_1 = \begin{bmatrix} 0 & -1 & 0 \\ 1 & 0 & 0 \\ 0 & 0 & 1 \end{bmatrix} \quad \bar{s}_2 = \begin{bmatrix} 1 & 0 & 0 \\ 0 & 0 & -1 \\ 0 & 1 & 0 \end{bmatrix}$$

Note that  $\bar{s}_i^2$  is a diagonal matrix which is equal to the identity up to multiplication by  $H$ , but isn’t exactly the identity. When a clean inverse is required we write  $\bar{s}_i = \bar{s}_i^{-1}$ . Most contractions will abstractly depend on the word and not the lift.

**Definition 10.8.** *The **longest word** in the Weyl Group  $\omega_0$  is the word in  $W$  with the longest reduced expression.*

The longest word has a well defined lift to the group  $\bar{\omega}_0$  and in our setup is antidiagonal alternating  $-1$  and  $1$  from the top right.

$$\bar{\omega}_0 = \begin{bmatrix} & & -1 \\ & 1 & \\ & -1 & \\ -1 & & \end{bmatrix}$$

We note this matrix (and the longest word) is independent of the particular reduced expression in  $s_i$  representing it.

**Remark 10.9.** *In  $\mathrm{SL}(n, \mathbb{C})$  the Weyl group is isomorphic to the symmetric group on  $n$  elements. Here  $s_i$  is the transposition exchanging  $i$  and  $i+1$  and  $\omega_0$  is the order reversing permuation.*

## 10.3 Generalized Minors

We can extend the fundamental weights to a **generalized minor** by pre/postcomposing with elements of the Weyl group.

**Definition 10.10.** *The generalized minor  $\Delta_i^{(u,v)}$  is the function defined on an element  $g$  by  $\Delta_i^{u,v}(g) = w_i(\bar{u}^{-1}g\bar{v})$  for each  $u, v$  in the Weyl group and each  $i$ .*

We note this function is independent of the choice of lifts of  $u$  and  $v$ . In  $\mathrm{SL}(n, \mathbb{C})$  we identified the weights with determinants of minors and the Weyl group with permutations. In this case  $\Delta_i^{u,v}$  is the determinant of the minor with rows  $u[1, \dots, i]$  and columns  $v[1, \dots, i]$ . We write  $\Delta_{u[1, \dots, i], v[1, \dots, i]}$  for the actual minor.

## 11 Bruhat Cell

We now have enough notation to define the Bruhat decomposition of a group.

**Definition 11.1.** For each element  $w \in W$  the **Bruhat cell** is the double coset  $BwB$

Recall that left/right multiplying by upper triangular matrices corresponds to row/column operations. Under this interpretation each Bruhat cell correspond to the permutation matrix that remains after row reducing a matrix of full rank. In  $\mathrm{SL}(n, \mathbb{C})$  there is a simple list of conditions for an element to belong to the Bruhat cell indexed by  $w$ .

**Theorem 11.2.** An element  $g \in \mathrm{SL}(n, \mathbb{C})$  belongs to the Bruhat cell  $BwB$  if

1. For  $i = 1, \dots, n-1$ ,  $\Delta_{u[1, \dots, i], [1, \dots, i]}(g) \neq 0$
2. For  $1 \leq i < j \leq n$ , if  $u(i) < u(j)$  then  $\Delta_{u[1, \dots, i] \cup \{j\}, [1, \dots, j]} = 0$

For the following examples we specialize to  $\mathrm{SL}(3, \mathbb{C})$  which is type  $A_2$ .

**Example 11.3.** Consider the Bruhat cell corresponding to the longest word  $s_1 s_2 s_1$ . This correspond to the order reversing permutation (in one line notation 321).

The first conditions on nonzero minors are then on  $g_{3,1}$  the bottom left entry and  $\begin{bmatrix} g_{21} & g_{22} \\ g_{31} & g_{22} \end{bmatrix}$ . There are no minors that are forced to vanish as the permutation never preserves the ordering on  $i < j$ .

**Example 11.4.** Now consider the Bruhat cell corresponding to the empty word. As a permutation this is the identity (in one line notation 123).

The nonvanishing minors are  $g_{11}$  the top left entry and  $\begin{bmatrix} g_{11} & g_{12} \\ g_{21} & g_{22} \end{bmatrix}$ . Now for each  $1 \leq i < j \leq 3$  the permutation preserves the order. So for  $i = 1$   $j = 2, 3$  and  $i = 2$   $j = 3$  the minor must vanish. When  $i = 1$  the corresponding minor is  $g_{j,1}$ . So we know  $g_{2,1} = g_{3,1} = 0$ . The final vanishing minor is

$$\det \begin{bmatrix} g_{11} & g_{12} \\ g_{31} & g_{32} \end{bmatrix} = g_{11}g_{32} - g_{12}g_{31} = g_{11}g_{32} - g_{12}0 = g_{11}g_{32}$$

For this minor to vanish and have  $g_{11} \neq 0$  we must have  $g_{32} = 0$ . In other words  $g$  is an upper triangular matrix with all diagonal entries nonzero as expected (the Bruhat cell corresponding to the empty word is  $B$ ).

**Remark 11.5.** As  $B^-$  is the transpose of  $B$  we can get analogous conditions for a matrix to belong to a Bruhat cell defined using  $B^-$  by swapping the row and column data.

**Definition 11.6.** A **double Bruhat cell** depends on the choice of two words  $u, v \in W$  and is the intersection  $G^{u,v} = B^+ u B^+ \cap B^- v B^-$ .

There are a few choices of word that are of special interest to us.

- The largest Bruhat cell is  $G^{\omega_0, \omega_0}$ . This is the “generic” cell in the group.
- The cell  $G^{e, \omega_0}$  is important in the study of full flag varieties. If we fix two flags as the standard and opposite flag  $\tau_+ = B, \tau_- = B^-$ , this cell consists of group elements  $g$  so that  $g\tau_-$  is a flag transverse to both  $\tau_+$  and  $\tau_-$ . In fact every flag transverse to both  $\tau_+$  and  $\tau_-$  is represented by such an element.

It is also convenient to look at the **reduced Double Bruhat Cell**  $L^{u,v} = N^+ u N^+ \cap B^- v B^-$ . This can be obtained from the full cell by an action of  $H$  and thus separates out the influence of  $H$  on the cell.

### 11.1 Parameterization of Double Bruhat Cells

Luzstig gave a parameterization of an open dense subset of  $L^{u,v}$  on a reduced expression for the word  $(u, v)$ . This is a map  $x : \mathbb{C}^{\ell(u)+\ell(v)} \rightarrow L^{u,v}$  given by

$$x(t_1, \dots, t_m) = \tilde{X}_{i_1}(t_1) \cdots \tilde{X}_{i_{n+m}}(t_{n+m})$$

$$\text{Here } \tilde{X}_i(t) = \begin{cases} X_i(t) & i \in v \\ \begin{bmatrix} I & & \\ & t^{-1} & 0 \\ & 1 & t \\ & & I \end{bmatrix} & i \in u \end{cases}.$$

**Example 11.7.** We return to  $G = \mathrm{SL}(3, \mathbb{C})$  and the cell  $G^{e, \omega_0}$ . As a reduced word we take  $s_1 s_2 s_1$ . Then the map  $x$  is

$$x_{121}(t_1, t_2, t_3) = \begin{bmatrix} 1 & t_1 & 0 \\ 0 & 1 & 0 \\ 0 & 0 & 1 \end{bmatrix} \begin{bmatrix} 1 & 0 & 0 \\ 0 & 1 & t_2 \\ 0 & 0 & 1 \end{bmatrix} \begin{bmatrix} 1 & t_3 & 0 \\ 0 & 1 & 0 \\ 0 & 0 & 1 \end{bmatrix} = \begin{bmatrix} 1 & t_1 + t_3 & t_1 t_2 \\ 0 & 1 & t_2 \\ 0 & 0 & 1 \end{bmatrix}$$

However if we use the reduced expression  $s_2 s_1 s_2$  we obtain the map

$$x_{212}(t_1, t_2, t_3) = \begin{bmatrix} 1 & t_2 & t_2 t_3 \\ 0 & 1 & t_1 + t_3 \\ 0 & 0 & 1 \end{bmatrix}$$

### 12 Cluster Structure

Recall that to describe a cluster structure it suffices to give a recipe for an initial seed (a quiver and associated functions). In this case the functions should be regular functions on the given double Bruhat cell  $G^{u,v}$ . The following recipe is from [BFZ05] and depends on a choice of reduced expression for the word  $(u, v)$  denoted  $\mathbf{i} = i_1 \cdots, i_{n+m}$ .

Let  $r$  be the rank of our Lie Group. The quiver will live in an  $r \times (n+m+r)$  grid with one node in each column. We index the columns  $-r, -(r-1), \dots, -1, 1, 2, \dots, m+n$ . The height of the node in column  $k > 0$  is index of the corresponding reflection  $i_k$ . The heights of the nodes in columns  $-k$  is  $k$ .

There are 3 classes of arrows we add to the quiver. To describe the classes we introduce the notation  $k^+$  which denotes the next index in  $\mathbf{i}$  such that  $|i_k| = |i_{k^+}|$ . If no such index exists take  $k^+ = m+n+1$  (larger than any possible index).

We also write  $\varepsilon(i_k)$  to denote the sign of  $i_k$  (whether the reflection belongs to  $u$  or to  $v$ ). We caution that  $u$  uses the negative values as we are most often interested in the  $e, \omega_0$  case. Consider two indices  $k$  and  $\ell$  with  $k < \ell$ .

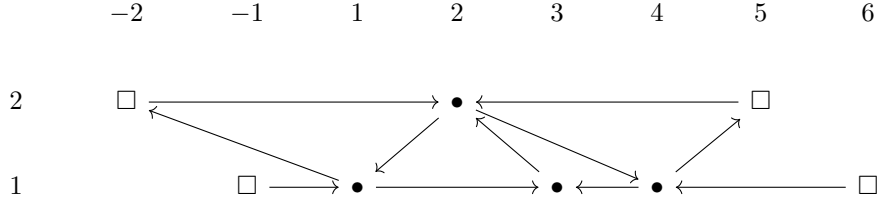
1. There is a **horizontal arrow** from  $k$  to  $\ell = k^+$  when  $\varepsilon(i_{k^+}) = 1$ . When  $\varepsilon(i_{k^+}) = -1$  the arrow is oriented from  $k^+$  to  $k$ .

2. There is an **inclined arrow** from  $\ell$  to  $k$  when  $\ell < k^+ < \ell^+$  and  $\varepsilon(i_\ell) = \varepsilon(i_{k^+}) = 1$  and  $i_k$  is adjacent to  $i_\ell$  in the Dynkin diagram. When  $\varepsilon(i_\ell) = \varepsilon(i_{k^+}) = -1$  the arrow is oriented from  $k$  to  $\ell$ .
3. There is an **inclined arrow** from  $\ell$  to  $k$  when  $\ell < \ell^+ < k^+$  and  $\varepsilon(i_\ell) = -\varepsilon(i_{\ell^+}) = 1$  and  $|i_k| = |i_\ell|$  in the Dynkin diagram. Similarly when  $\varepsilon(i_\ell) = -1$  we reverse the orientation of the arrow in this case.

We take the first and last node at each “height” as frozen nodes.

While this definition is very technical an example can make everything clearer.

**Example 12.1.** We continue looking at  $G = \mathrm{SL}(3, \mathbb{C})$  and consider the largest cell  $G^{\omega_0, \omega_0}$ . As reduced expression we take  $\mathbf{i} = (1, 2, 1, -1, -2, -1)$ .



**Remark 12.2.** This quiver is very similar to the quiver for  $Gr(3, 6)$ , it is only missing two frozen nodes. This is due to the fact that a matrix in  $A \in \mathrm{SL}(3, \mathbb{C})$  determines a 3 plane in  $\mathbb{C}^6$  via  $I|A$ . This plane has two Plücker coordinates equal to zero corresponding to the empty and full minors of  $A$ .

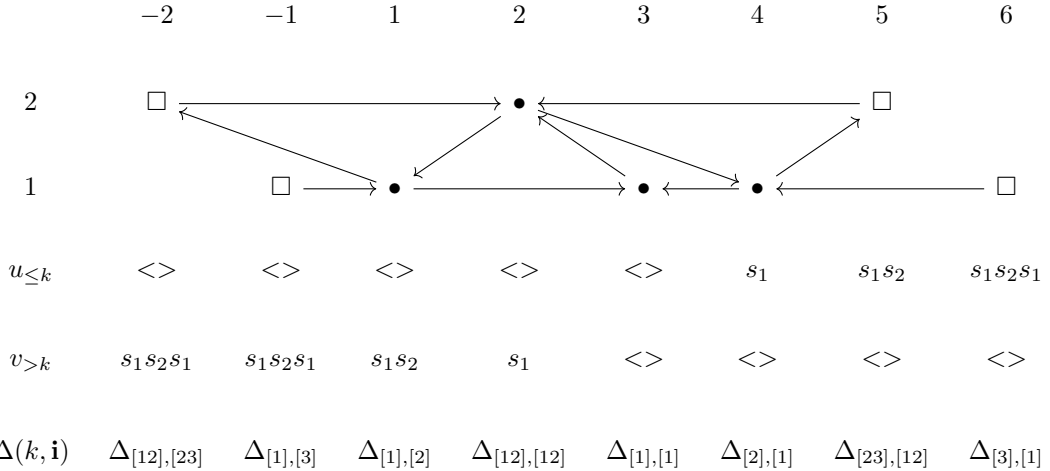
It now remains to describe the functions associated to each node. These will be generalized minors where the Weyl group elements are given by subwords of  $\mathbf{i}$ . We require a little more notation:

$$u_{\leq k}(\mathbf{i}) = \prod_{\ell=1 \dots k, \varepsilon(i_\ell)=-1} s_{|i_\ell|} \quad v_{>k} = \prod_{\ell=m+n \dots k+1, \varepsilon(i_\ell)=1} s_{|i_\ell|}$$

In words  $u_{\leq k}$  is the product of generators of  $u$  ( $\varepsilon = -1$ ) in the first  $k$  symbols and  $v_{>k}$  is the reversed product of generators of  $v$  ( $\varepsilon = 1$ ) after the first  $k$  symbols.

The function associated to node  $k$  of the quiver  $\Delta(k, \mathbf{i}) = \Delta_{u_{\leq k}, v_{>k}}^{|i_k|}$ .

**Example 12.3.** We continue our top Bruhat cell in  $\mathrm{SL}(3, \mathbb{C})$  with  $\mathbf{i} = (1, 2, 1, -1, -2, -1)$ . We recall that under the isomorphism of the Weyl group with the symmetric group  $s_1s_2s_1 \mapsto 321$ ,  $s_1s_2 \mapsto 231$ , and  $s_1 \mapsto 213$ .



Note that the frozen variables are exactly the nonvanishing conditions to be in  $G^{\omega_0, \omega_0}$ .

**Example 12.4.** We now consider a smaller example of  $G^{e, \omega_0}$  in  $\mathrm{SL}(3, \mathbb{C})$ . We take  $\mathbf{i} = 121$ .

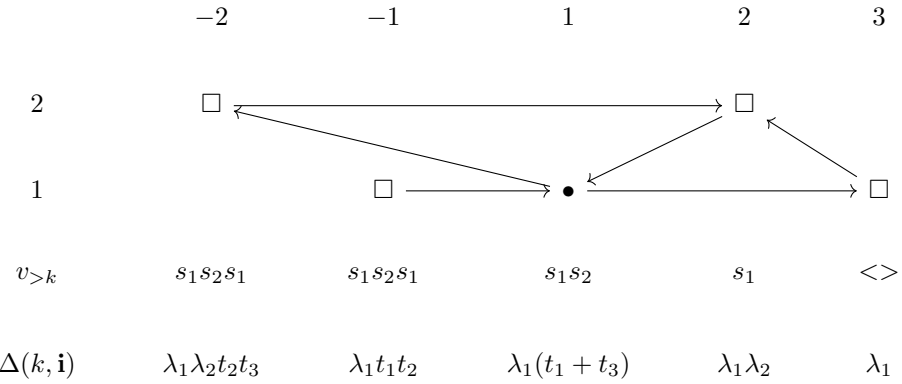
Our parameterization of  $L^{e,\omega_0}$  gave us a map whose image is

$$\begin{bmatrix} 1 & t_1 + t_3 & t_1 t_2 \\ & 1 & t_2 \\ & & 1 \end{bmatrix}$$

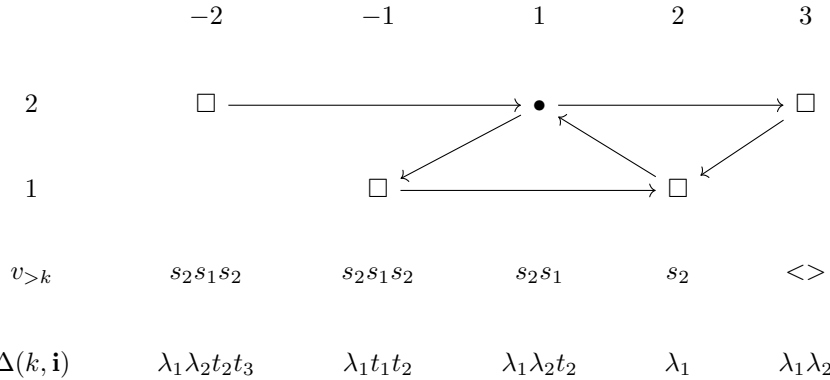
To obtain a full parameterization of  $G^{e,\omega_0}$  we can left multiply by a generic element of the torus  $\begin{bmatrix} \lambda_1 & & \\ & \lambda_2 & \\ & & \lambda_1^{-1} \lambda_2^{-1} \end{bmatrix}$  to obtain:

$$\begin{bmatrix} \lambda_1 & \lambda_1(t_1 + t_3) & \lambda_1 t_1 t_2 \\ & \lambda_2 & \lambda_2 t_2 \\ & & \lambda_1^{-1} \lambda_2^{-1} \end{bmatrix}$$

The recipe then gives



**Example 12.5.** We now compute a seed for the same double Bruhat cell with a new word  $\mathbf{i} = s_2s_1s_2$ .



Note that the previous two examples are related by cluster mutation! In fact every reduced expression is connected by a series of mutations. We can confirm this by realizing the “local” moves on words as mutations.

- Two moves inside words of the same sign correspond to the same quiver.
- Three moves correspond to quiver mutation at the initial index of the 3 move.

To fully verify this gives a cluster structure on the coordinate ring we must verify the preconditions of the Starfish Lemma (Theorem 8.1). The first to check is that every mutation produces a regular function. By the analysis above every mutation that corresponds to a 3 move is fine. The other mutations require a computation similar to the confirmation that the “exotic” coordinate in  $\text{Gr}(3, 6)$  is regular.

Next we must check that the space of “double zeros” has codimension at least 2. This is true as all of the minors are irreducible elements and one can confirm the mutated minors from a given word maintain this property.

Finally we must confirm that we cover the entire ring. This can be seen as every matrix entry is obtained by some choice of reduced expression of the longest word.

## Part V

# Lecture Five: Higher Teichmuller Theory

In this lecture our goal will be to study representations  $\pi_1 S \rightarrow G$  for  $S$  a bordered surface and  $G$  a split semisimple Lie Group. While the techniques described will apply in this generality we will focus on  $G$  simple and give explicit definitions for  $G = \mathrm{SL}(n, \mathbb{R})$ .

The cluster structure we build will be in analogy to our discussion of the cluster structure on the space of hyperbolic structures on a surface in Lecture I.

## 13 Framed Representations

In Lecture I we described hyperbolic structures on a surface via the developing/holonomy maps into  $\mathbb{H}^2$ . A key ingredient was that the points on the boundary of hyperbolic space controlled the representation of the fundamental group and the image of the surface.

In order to generalize this picture we recall that points in boundary of hyperbolic space correspond to points in  $\mathbb{P}^1\mathbb{R}$ . These can be interpreted as lines in  $\mathbb{R}^2$  which are the same as flags in  $\mathrm{SL}(2, \mathbb{R})$ .

Fix a Lie group  $G$  with  $B$  a Borel subgroup and  $N$  its unipotent radical.

**Definition 13.1.** A **framed representation** from a bordered surface  $S$  into  $G$  is a representation  $\rho : \pi_1(S) \rightarrow G$  and a choice of flag  $F_p \in G/B$  for each marked point and puncture of  $S$  such that  $\rho(\gamma).F_p = F_p$  for any curve  $\gamma$  homotopic to a puncture  $p$ .

**Definition 13.2.** A **decorated representation** is a framed representation where the flags are chosen in the set of decorated flags  $G/N$ .

When  $S$  is hyperbolic we will be able to describe a cluster structure on the space of decorated representations of  $S$ . As in the hyperbolic case we build this cluster structure out of ideal triangles. As such we must focus on the representations of triangle/disk with 3 marked points into  $G$ . As  $\pi_1$  of a disk is trivial, all of the data of a decorated representation is in the choice of flags. In the hyperbolic case it sufficed to chose distinct points on  $\mathbb{H}$ . In other groups we need not just distinct flags, but for the flags to be pairwise transverse.

### 13.1 Transverse Flags

To continue we need to describe several ways to think about flags, each of which has an equivalent definition of transversality. The first way is to describe a flag as an equivalence class of matrices. This is the notation  $G/B$  or  $G/N$  we have been using. The other common definition of a flag is as a nested sequence of subspaces. From a matrix representative with columns  $v_1, \dots, v_n$  the corresponding subspaces are

$$\langle v_1 \rangle \subseteq \langle v_1, v_2 \rangle \subseteq \langle v_1, v_2, v_3 \rangle \subseteq \cdots \subseteq \langle v_1, \dots, v_n \rangle$$

In this case decorations correspond to a choice of basis vector in each new subspace  $V^{i+1}/V_i$ .

On a flag manifold we fix two special flags, the **standard flag**  $\tau_+ = [B]$  and the opposite flag  $\tau_- = [B^-]$ .

**Example 13.3.** In  $\mathrm{SL}(n, \mathbb{R})$ ,  $\tau_+$  is represented by identity matrix. As a series of nested subspaces

$$\tau_+ = \langle e_1 \rangle \subseteq \langle e_1, e_2 \rangle \subseteq \cdots \subseteq \langle e_1, e_2, \dots, e_n \rangle.$$

The opposite flag  $\tau_-$  is represented by reversed identity matrix. As a series of nested subspaces

$$\tau_- = \langle e_n \rangle \subseteq \langle e_n, e_{n-1} \rangle \subseteq \cdots \subseteq \langle e_n, \dots, e_1 \rangle.$$

The diagonal action by left multiplication of  $G$  on pairs of flags splits into a number of orbits. There is a unique open orbit of this action.

**Definition 13.4.** *Two flags are **transverse** if they belong to this open orbit.*

With a little more work one can show that each orbit is indexed by an element  $w$  of the Weyl group. In other words there is a  $g$  taking any pair of flags  $(F_1, F_2)$  to  $(\tau_+, w\tau_+)$ . The open orbit corresponds to  $\omega_0$  the longest word in the Weyl group.

**Definition 13.5.** *The  **$w$ -distance** between two flags  $(F_1, F_2)$  is the  $w$  identifying the orbit. Two flags are **transverse** when the  $w$  distance is  $\omega_0$ .*

Note that  $w(F_1, F_2) = w(F_2, F_1)^{-1}$  and so depends on the order of flags in general. However  $\omega_0$  is its own inverse and so transversality is a symmetric condition.

Finally if we view our flags as a series of nested subspaces (generated by columns of our matrix representatives) transversality corresponds to disjointness of subspaces.

**Definition 13.6.** *Let  $F_1 = F_1^{(1)} \subseteq F_1^{(2)} \subseteq \dots \subseteq F_1^{(n)}$  and  $F_2 = F_2^{(1)} \subseteq F_2^{(2)} \subseteq \dots \subseteq F_2^{(n)}$ . Then  $F_1$  and  $F_2$  are **transverse** if whenever  $i + j = n$ ,  $F_1^{(i)} \oplus F_2^{(j)} = V$ .*

**Remark 13.7.** *The standard and opposite flags are always transverse.*

We now consider a triple of transverse flags. In the last lecture we looked at the double Bruhat cell  $G^{e, \omega_0}$ . In  $\mathrm{SL}(n, \mathbb{R})$  we saw this corresponds to upper triangular matrices whose antiprinciple minors are nonzero.

**Claim 13.8.** *Every flag transverse to  $\tau_+$  and  $\tau_-$  is represented by  $g\tau_-$  for  $g \in G^{e, \omega_0}$ .*

*Proof.* In  $\mathrm{SL}(n, \mathbb{R})$  we can perform an explicit computation. A simple test for subspaces to combine to the whole space is to take the wedge product of basis for each space and check this doesn't vanish. Thus testing if a flag represented by a matrix  $g$  is transverse to the standard flag is equivalent to the nonvanishing of minors of the form  $\Delta_{[1,k],[n-k+1,n]}$ . Each matrix  $g\tau_-$  is "reverse upper triangular" and thus all these minors are products of the antidiagonal. This is the product of the diagonal in  $B$  which is always nonzero. Similarly the conditions to be transverse to the opposite flag correspond to the nonvanishing of  $\Delta_{[1,k],[1,k]}$ . This corresponds to the antiprinciple minors of  $g \in G^{e, \omega_0}$  which are assumed not to vanish.  $\square$

**Remark 13.9.** *The element  $g \in G^{e, \omega_0}$  representing the flag is not unique. If fact if  $g = nh$  for  $n \in N$  and  $h \in H$  we have  $nh\tau_- = nh\omega_0 B = n\omega_0 h^{-1} B = n\omega_0 B$ .*

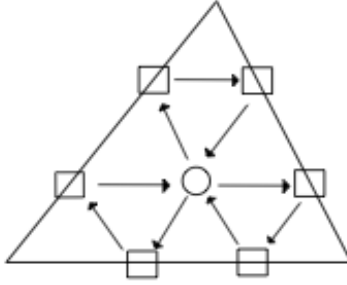
So as undecorated flags each triple corresponds to a unique element  $n \in L^{e, \omega_0}$  the reduced double Bruhat cell.

However to get the nicest cluster structure we want to look at decorated flags (in analogy with  $\mathrm{SL}(2, \mathbb{R})$ ). In this case the orbits of pairs of flags split further based on the relative scaling of the flags. In other words  $(F_1, F_2) \mapsto (\tau_+, h\tau_-)$  for some  $h \in H$ .

**Definition 13.10.** *The  **$h$ -distance** between a pair of transverse decorated flags  $(F_1, F_2)$  is the unique  $h \in H$  such that there is a  $g \in G$  such that  $g(F_1, F_2) = (\tau_+, h\tau_-)$ .*

This is the information we need to obtain a cluster structure on configurations of transverse triples of decorated flags. First we pick an element of  $g$  that sends 3 arbitrary flags  $(F_1, F_2, F_3)$  to  $(\tau_+, h\tau_-, b\tau_-)$  where we know  $b \in G^{e, \omega_0}$ . The cluster structure on  $G^{e, \omega_0}$  parameterizes the element  $b$  but doesn't take into account the first  $h$  or the choice of which flags to send to the standard/opposite flags. As such we need to "symmetrize" the double Bruhat cell recipe by adding  $\mathrm{rank}(G)$  many frozen vertices to account for  $h$ . For full details of the recipe for arbitrary groups see [GS22].

**Example 13.11.** *The seed for  $\mathrm{SL}(3, \mathbb{R})$  with  $\omega_0 = s_1 s_2 s_1$  is*



### 13.2 Counting Components of Triples of Transverse Flags

The cluster structure can help us understand the topology of the space of triples of transverse flags,  $T$ . At least it provides a nice tool for counting/identifying components. Each seed of the cluster algebra provides a continuous invertible map from  $(\mathbb{R} \setminus \{0\})^N \rightarrow T$ . Thus counting components of  $T$  amounts to deciding which components of  $(\mathbb{R} \setminus \{0\})^N$  are glued together.

**Definition 13.12.** A (*generalized*) *orthant* is a component of  $(\mathbb{R} \setminus \{0\})^N$ . Each orthant is indexed by a list of signs for each node of the quiver.

Since the image of the set where multiple cluster variables in a seed and its neighbors are zero is codimension 2, this set cannot change connectivity in the image. Thus it suffices to consider where exactly one cluster variable is zero to determine which components glue together.

We now define a linear group acting on the space of signs. We will show the orbits of this group correspond to components in the image. Further the orbits of the group are easy to compute, thus the components are easily identified.

For each mutable node  $i$  define the “transvection”,  $\tau_i : \mathbb{F}_2^N \rightarrow \mathbb{F}_2^N$

$$\tau_i(\xi)_j = \begin{cases} \xi_j & j \neq i \\ \xi_i + \sum_{k \rightarrow i} \xi_k + \sum_{i \rightarrow k} \xi_k & j = i \end{cases}$$

Let  $\Gamma$  be the group generated by  $\tau_i$  for each mutable node  $i$ .

**Theorem 13.13.** The orbits of  $\Gamma$  correspond exactly to the components of  $T$ .

*Proof.* The key idea is that the mutable variables being zero in one seed doesn’t imply that all the variables in another seed are zero. Thus we should glue together orthants which are connected in neighboring seeds. It suffices to look at two orthants that differ by a single sign at position  $i$  for some mutable node. If these two orthants glue together that means that  $a_i = 0$  while its mutated variables  $a'_i \neq 0$ . However the mutation relation is

$$a_i a'_i = \prod_{j \rightarrow i} a_j + \prod_{i \rightarrow k} a_k$$

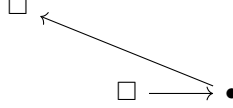
Thus for  $a_i$  to be 0, the left hand side of the mutation relation is zero. This implies  $\prod_{j \rightarrow i} a_j$  and  $\prod_{i \rightarrow k} a_k$  must

have opposite signs. In  $\mathbb{F}_2$  this corresponds to  $\sum_{j \rightarrow i} a_j + \sum_{i \rightarrow k} a_k = 1$  and so  $\tau_i(\mathbf{a})$  changes the sign at  $i$ . Thus two orthants that are glued together in the image belong to the same orbit.

Conversely if  $\tau_i$  changes the sign at  $i$  this implies that  $\prod_{j \rightarrow i} a_j$  and  $\prod_{i \rightarrow k} a_k$  have opposite signs. Using the seed obtained by mutating at  $i$  we find an element in the image so the right hand side of the mutation relation vanishes. By wiggling this element slightly we find neighbors with  $a_i > 0$  and  $a_i < 0$  and so the corresponding orthants are in the same component.  $\square$

**Remark 13.14.** There was a coincidence here that the frozen variables of the cluster structure are exactly the conditions for the flags to be transverse. In a general cluster algebra this method counts components where the frozen variables are nonzero. However this is only meaningful geometrically when the nonvanishing of the frozen variables is a natural condition on the space in interest.

**Example 13.15.** We will count the components of triples of transverse flags in  $\mathrm{SL}(3, \mathbb{R})$ . In order to get a cluster structure we can chose decorations so that the flags are  $(\tau_+, \tau_-, u\tau_-)$  for  $u \in L^{e, \omega_0}$  the reduced double Bruhat cell. This means we take the frozen variables on the far right of the double Bruhat cell construction to be 1. What remains is



We now need to compute orbits under the group action. Label the vertices from left to right  $v_1, v_2, v_3$ . As we have one mutable vertex  $v_3$  our group is generated by  $\tau_3(a_1, a_2, a_3) = (a_1, a_2, a_3 + a_1 + a_2)$ . Thus  $\tau_3$  acts nontrivially only when  $a_1$  and  $a_2$  have different signs. So the six orbits are:

$$(0, 0, 0) \quad (0, 0, 1) \quad (1, 1, 0) \quad (1, 1, 1) \quad (1, 0, 0) - (1, 0, 1) \quad (0, 1, 0) - (0, 1, 1)$$

One can perform a similar analysis to find the number of components in  $\mathrm{SL}(4, \mathbb{R})$  is 20 and in  $\mathrm{SL}(5, \mathbb{R})$  is 52. For very large  $n$  computing via the group action becomes infeasible. Recall that the cluster structure for triples of flags in  $\mathrm{SL}(n, \mathbb{R})$  has the same number of mutable nodes as the length of the longest word  $\binom{n}{2}$ . Thus the number of orthants is  $O(2^{\binom{n}{2}})$  which is very large.

Fortunately there is theorem that classifies orbits for large enough quivers.

**Theorem 13.16.** If the mutable portion of the quiver contains an  $E_6$  as an induced subgraph then the number of orbits of the group action is  $2 \cdot 2^r + d$  where  $r$  is the number of frozen variables and  $d$  is the number of singleton orbits.

For full proof see [Zel00]. As a brief sketch, we know that the sign of each frozen variable is invariant under group action. We then can analyze each “slice” of orthants over a fixed list of frozen signs. The orbits come in two flavors, singleton and nonsingleton. When the quiver contains this  $E_6$  we can show that each slice has exactly 2 nonsingleton orbits which are distinguished by the value of a function  $Q$ . We can compute  $Q$  as the  $\mathbb{F}_2$  form given by  $Q(\mathbf{a}) = \sum a_i + \sum_{i \rightarrow j} a_i a_j$ . It is a simple computation to verify that  $Q$  is invariant under the group action. As  $\tau_i$  can only change the sign at  $i$  it suffices to look at the portion of  $Q(\mathbf{a})$  that depends on  $a_i$

$$\begin{aligned} & a_i + \sum_{j \rightarrow i} a_i a_j + \sum_{i \rightarrow k} a_i a_k \\ & \mapsto \left( a_i + \sum_{j \rightarrow i} a_j + \sum_{i \rightarrow k} a_k \right) + \sum_{j \rightarrow i} \left( a_i + \sum_{j \rightarrow i} a_j + \sum_{i \rightarrow k} a_k \right) a_j + \sum_{i \rightarrow k} \left( a_i + \sum_{j \rightarrow i} a_j + \sum_{i \rightarrow k} a_k \right) a_k \\ & = a_i + \sum_{j \rightarrow i} a_j + \sum_{i \rightarrow k} a_k + \left( \sum_{i \rightarrow k} a_k \right)^2 + \sum_{i \rightarrow k} a_k + \left( \sum_{j \rightarrow i} a_j \right)^2 + \sum_{j \rightarrow i} a_j + \sum_{j \rightarrow i} \sum_{i \rightarrow k} a_j a_k + \sum_{i \rightarrow k} \sum_{j \rightarrow i} a_j a_k \\ & = a_i + \sum_{j \rightarrow i} a_j + \sum_{i \rightarrow k} a_k \end{aligned}$$

The analysis of singleton orbits is slightly trickier. The key fact is that when a slice has singleton orbits it has the same number of singleton orbits as the slice with all frozen variables positive. Thus it suffices to

count how many slices can possibly have a singleton orbit.

In the specific case of full flag manifolds, the count of singleton orbits is easier. Each singleton component corresponds to a choice of “positive” in each root space. There is one frozen variable for each root space and thus  $2^r$  possible singleton components.

### 13.3 Alternate Recipe For $\mathrm{SL}(n, \mathbb{R})$

For  $\mathrm{SL}(n, \mathbb{R})$  there is an alternate description for a seed of triples of transverse decorated flags. This is equivalent to the seed given by the word  $12 \cdots n12 \cdots (n-1) \cdots 121$ . The nodes of this seed naturally lie inside a triangle. For each side of the triangle draw  $n-1$  lines parallel to it through the interior of the triangle. These should be chosen to such that the lines meet at triple intersections. Each node is placed on a triple intersection and is indexed by the number of lines from each base. These are three numbers  $(i, j, k)$  such that the sum  $i + j + k = n$  and each index is between 0 and  $n-1$ . Note that triples with a single zero belong to the outer edge of triangle and we have no points with two zeros.

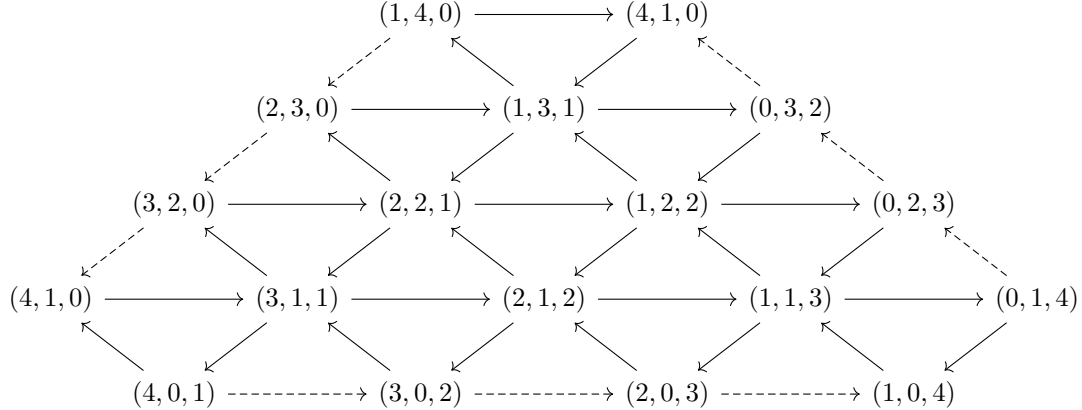
The quiver has edge connecting  $(i, j, k)$  out to  $(i-1, j, k+1), (i, j+1, k-1), (i+1, j-1, k)$  and correspondingly in from  $(i+1, j, k-1), (i, j-1, k+1), (i-1, j+1, k)$ . Under this construction each induced cycle is an oriented 3 cycle. Moreover the arrows parallel to each side of the triangle are oriented from left to right when looking into the triangle from that edge.

Let the three flags associated to the triangle have basis given  $F_1 = (u_1, \dots, u_n)$ ,  $F_2 = (v_1, \dots, v_n)$  and  $F_3 = (w_1, \dots, w_n)$ . We then define the function  $p_{ijk} = (u_1 \wedge \cdots \wedge u_i) \wedge (v_1 \wedge \cdots \wedge v_j) \wedge (w_1 \wedge \cdots \wedge w_k)$ . This is an  $n$  wedge in  $n$  dimensional space which isomorphic to  $\mathbb{R}$  after having fixed a standard basis of  $\mathbb{R}^n$  once and for all.

We define the frozen nodes to be the nodes on the border of the triangle. As mentioned these are the nodes with one index 0. It will be helpful later to take the arrows between frozen nodes on the same edge of the triangle as half weight (represented by a dashed edge).

**Remark 13.17.** For  $\mathrm{SL}(2, \mathbb{R})$  this construction places an oriented clockwise cycle in the triangle agreeing with construction for hyperbolic structures on a surface.

**Example 13.18.** The quiver for  $\mathrm{SL}(4, \mathbb{R})$  is given below.



**Remark 13.19.** Note that the cluster functions on the edges of the triangle only depend on the two flags on that edge. This remains true for the other simple Lie groups as under the other recipe these functions describe the  $h$  distance between the two flags.

## 14 Amalgamating

We now describe the cluster structure for decorated representations of a bordered surface. First we take an ideal triangulation of the surface. To each triangle we attach a seed as described for a triple of transverse

flags (using the transverse flags from the framing on the representation). These seeds are then glued together by a **amalgamation**.

**Definition 14.1.** *The amalgamation of two seeds is given by identifying frozen nodes with identical functions. Any edges between these identified frozen variables are added. Then the newly glued frozen variables are treated as unfrozen in the new seed.*

**Remark 14.2.** *Half edges between the frozen nodes will either become full edges or cancel after amalgamating.*

As the functions on the edges of each triangle only depend on the flags assigned to the endpoints each seed will amalgamate together to form a seed on the entire surface with frozen nodes on the boundary of the surface. It remains to show this construction is independent of the chosen triangulation. As before we can relate triangulations by a sequence of local moves, (flipping the interior diagonal of a square). To verify the cluster structure is the same under either triangulation we must provide a sequence of mutations. Such sequences are computed explicitly in [Gil21]. However for  $\text{SL}(3, \mathbb{R})$  the sequence is short enough to demonstrate explicitly.

**Example 14.3.** *For  $\text{SL}(3, \mathbb{R})$  the mutation sequence corresponding to retriangulation with the explicit seed described in Section 13.3 is to first mutate at both nodes on the interior edge, then to mutate both the remaining two nodes. See Figure 15. To see we obtain the correct functions we will explicitly compute one mutation. Label the basis for the four flags  $\mathbf{u}, \mathbf{w}, \mathbf{z}, \mathbf{v}$  reading clockwise around the square. Mutation at the node closest to  $\mathbf{w}$  is given by*

$$w_1 \wedge w_2 \wedge v_1 \cdot ?? = w_1 \wedge w_2 \wedge u_1 \cdot v_1 \wedge w_1 \wedge z_1 + u_1 \wedge v_1 \wedge w_1 \cdot w_1 \wedge w_2 \wedge z_1$$

Note that each of these forms contains  $w_1$ . If we quotient  $\mathbb{R}^3$  by  $\langle w_1 \rangle$  what remains is 4 vectors in  $\mathbb{R}^2$  which is the setting of the short Plucker relation. Thus the mystery function is  $w_1 \wedge u_1 \wedge z_1$  as expected for the horizontal triangulation.

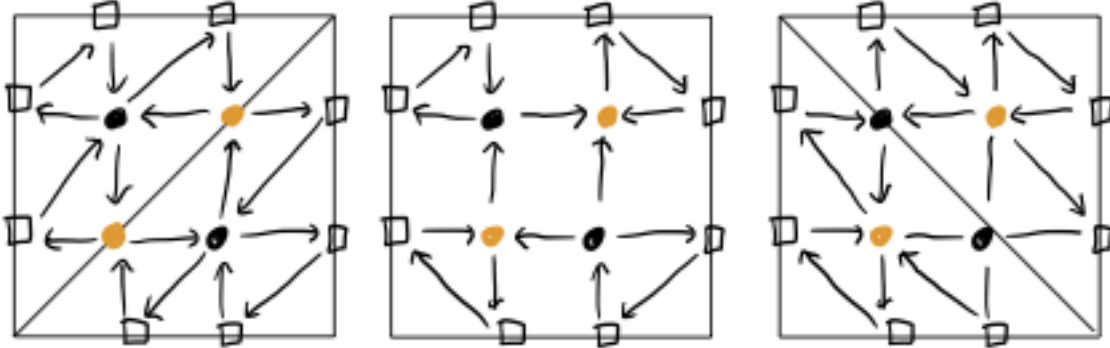


Figure 15: The mutation sequence flipping an edge in  $\text{SL}(3, \mathbb{R})$ .

**Remark 14.4.** *We are lucky in the  $\text{SL}(n, \mathbb{R})$  that the seed described is rotationally symmetric and the functions clearly only depend on the cyclic order of the quiver. However the general construction involves choosing two of the flags to send to  $(\tau_+, h\tau_-)$ . As such in the other cases one also needs to provide a mutation sequence connecting the seeds obtained by “breaking the symmetry” along a different edge.*

## 14.1 Reconstructing Representations

For each triangle make hexagon graph (oriented so edges along angles go counter clockwise). Deform any loop on the surface onto this graph. Follow the loop picking up factor of a matrix for each edge.

Factors come in two varieties, angles and edges.

Angle moves correspond to the matrix that moves  $\tau_-$  to  $u\tau_-$  and keeps  $\tau_+$  fixed. In other words  $u$ .

In  $\text{PSL}(2, \mathbb{R})$  this depends on the length of the horocycle trapped inside the triangle.

$$\begin{bmatrix} 1 & \frac{b}{ac} \\ & 1 \end{bmatrix}$$

The edge moves correspond to trading the roles of  $\tau_+$  and  $h\tau_-$ . In  $\text{PSL}(2, \mathbb{R})$  this is:

$$\begin{bmatrix} & h \\ -h^{-1} & \end{bmatrix}$$

Note that the image is the result of multiplying these matrices in order left to right as we traverse the path. This is because in order to apply the next element we first have to move back to the standard triple which has the effect of conjugating by the element so far.

$$p \cdot (\tau_+, h_1\tau_-, uh_2\tau_-) \mapsto pf_k p^{-1} \cdot p \cdot (\tau_+, h_1\tau_-, uh_2\tau_+) = pf_k \cdot (\tau_+, h_1\tau_-, uh_2\tau_+)$$

One can check that the trivial loop inside a triangle maps to a trivial element as does moving back and forth along an edge gluing two triangles together.

Furthermore when the cluster coordinates are positive, each  $u$  mapping the flags is “positive” as well. This “positive” boundary map is key to proving that the image representation is discrete. Intuitively each element moves at least a positive amount and the composition moves can’t double back on themselves without literally being trivial.

We can also show that such elements are faithful, only trivial loops are mapped to the identity.

**Example 14.5.** We can look at the punctured torus with representations into  $\text{PSL}(2, \mathbb{R})$  as an example. The horizontal loop is given by

$$H = (G_1^{23})^{-1} S_b^{-1} G_3^{41} S_a^{-1} = \begin{bmatrix} -\frac{c^2}{ab} - \frac{a}{b} & \frac{c}{a^2} \\ c & -\frac{b}{a} \end{bmatrix}$$

## 15 Coordinates on Undecorated Representations

In many geometric applications, decorated flags are not as natural as undecorated flags. We saw this with hyperbolic structures where decorated flags involved choosing a horocycle in addition to a point on the boundary. We also had some natural coordinates in this case which are cross ratios.

### 15.1 Recall Cross Ratio as ratio of lambda lengths

We are able to realize the cross ratio as a product of two horocycle lengths. See Section 3.2 for details. In this way each cross ratio is written as a ratio of four lambda lengths (there is cancellation of the lambda length in the center).

### 15.2 Recall Generalized X Coordinate Definition

Key fact: Can always write X coordinate as a ratio of A-coordinates. This ratio is invariant under changing decoration.

Mutation changes neighbors as well.

**Example 15.1.** Look at seed for  $\text{PSL}(3, \mathbb{R})$  on a square. On glued edge get cross ratios. Also get a function in the center of each triangle. This is a ratio of 3 coordinates over 3 coordinate called the **triple ratio**.

### 15.3 Poisson Structure on X space

There is a natural Poisson structure on the X coordinates.

**Definition 15.2.** A **Poisson bracket** on an algebra  $V$  is an alternating bilinear map  $\{-, -\} : V \times V \rightarrow V$  such that

$$\text{Leibniz's Rule: } \{fg, h\} = \{f, h\}g + f\{g, h\}$$

$$\text{Jacobi identity: } \{f, \{g, h\}\} + \{g, \{h, f\}\} + \{h, \{f, g\}\} = 0$$

**Remark 15.3.** The Leibniz rule implies that  $\{f^n, g\} = n\{f, g\}f^{n-1}$  when  $n \neq 1$ . In particular  $\{f^{-1}, g\} = -\{f, g\}f^{-2}$ .

These brackets occur naturally in Symplectic geometry. In this case the Poisson bracket of functions corresponds to the Lie bracket of the corresponding Hamiltonian vector fields.

Given a seed  $(Q, \mathbf{x})$  for a X type cluster algebra we let  $\varepsilon_{ij}$  be the adjacency matrix associated to  $Q$ . We then define a bracket on X-coordinates as follows:

$$\{x_i, x_j\} = \varepsilon_{ij}x_i x_j$$

The key fact to check is that this definition is mutation invariant and thus makes sense on the whole space of  $X$  coordinates. This amounts to a computation one case of which we show here. Let  $(Q', \mathbf{x}')$  be the seed obtained by mutating at  $i$ . Let  $j$  be an index so  $i \rightarrow j$  in  $Q$ . In other words  $\varepsilon_{ij} = 1$  and  $\varepsilon'_{ij} = -1$ .

In  $Q'$  we compute  $\{x'_i, x'_j\} = -x'_i x'_j$ .

If we write  $\mathbf{x}'$  in terms of  $\mathbf{x}$  we see  $x'_i = x_i^{-1}$  and  $x'_j = x_j(1 + x_i)$ . Thus

$$\begin{aligned} \{x'_i, x'_j\} &= \{x_i^{-1}, x_j(1 + x_i)\} \\ &= -\{x_i, x_j(1 + x_i)\}x_i^{-2} \\ &= -\{x_i, x_j\}x_i^{-2} - \{x_i, x_j x_i\}x_i^{-2} \\ &= -\{x_i, x_j\}x_i^{-2} - \{x_i, x_i\}x_j x_i^{-2} - \{x_i, x_j\}x_i^{-1} \\ &= -x_i^{-1}x_j - x_j \\ &= -x_j(1 + x_i) \\ &= -x'_j x'_i \end{aligned}$$

A similar computation shows the bracket is preserved between edges going into  $i$  as well.

**Remark 15.4.** This bracket is very similar to the form used to distinguish components in Section 13.2.

**Definition 15.5.** A **Casimir element** is an element that has trivial bracket with every other element.

**Lemma 15.6.** If  $\mathbf{v}$  is a null vector of the adjacency matrix of  $Q$  then the element  $\prod x_i^{v_i}$  is a Casimir element.

*Proof.* This is again a small computation. If we take any basis function  $x_j$  the bracket is

$$\{x_j, \prod x_i^{v_i}\} = \sum_i \{x_j, x_i^{v_i}\} \prod_{k \neq i} x_k^{v_k} = \sum_i v_i \{x_j, x_i\} x_i^{v_i-1} \prod_{k \neq i} x_k^{v_k} = \sum_i v_i \varepsilon_{ji} x_j \prod_k x_k^{v_k} = \left( \sum_i v_i \varepsilon_{ji} \right) x_j \prod_k x_k^{v_k}$$

The coefficient is the inner product of a row of the adjacency matrix with  $\mathbf{v}$  which is assumed to be 0 as needed.  $\square$

**Example 15.7.** For  $Q$  a directed path in  $A_3$   $1 \rightarrow 2 \rightarrow 3$  there is a unique generator for the Casimir element  $x_1 x_3$ .

**Example 15.8.** There are no Casimir elements in  $A_2$ .

In general there is a unique generator for the Casimir elements in  $A_{2n-1}$  consisting of the product of  $n$  commuting X coordinates. In fact the X coordinates themselves can be considered the Casimir elements for  $A_1$ .

## References

- [BFZ05] Arkady Berenstein, Sergey Fomin, and Andrei Zelevinsky, *Cluster algebras. III. Upper bounds and double Bruhat cells*, Duke Math. J. **126** (2005), no. 1, 1–52. MR2110627
- [FST08] Sergey Fomin, Michael Shapiro, and Dylan Thurston, *Cluster algebras and triangulated surfaces. I. Cluster complexes*, Acta Math. **201** (2008), no. 1, 83–146. MR2448067
- [FT18] Sergey Fomin and Dylan Thurston, *Cluster algebras and triangulated surfaces Part II: Lambda lengths*, Mem. Amer. Math. Soc. **255** (2018), no. 1223, v+97. MR3852257
- [FWZ21a] Sergey Fomin, Lauren Williams, and Andrei Zelevinsky, *Introduction to cluster algebras. chapter 6*, 2021.
- [FWZ21b] ———, *Introduction to cluster algebras. chapters 1-3*, 2021.
- [FWZ21c] ———, *Introduction to cluster algebras. chapters 4-5*, 2021.
- [FZ03] Sergey Fomin and Andrei Zelevinsky, *Cluster algebras. II. Finite type classification*, Invent. Math. **154** (2003), no. 1, 63–121. MR2004457
- [Gil21] S Gilles, *Fock–goncharov coordinates for semisimple lie groups*, PhD thesis, 2021. Available at <https://drum.lib.umd.edu/items/1291b8a6-f983-4563-9de6-a491293e6386>.
- [GS22] Alexander Goncharov and Linhui Shen, *Quantum geometry of moduli spaces of local systems and representation theory*, 2022.
- [KG21] Dani Kaufman and Zachary Greenberg, *Cluster modular groups of affine and doubly extended cluster algebras*, arXiv:2107.10334 (2021).
- [LZ98] Bernard Leclerc and Andrei Zelevinsky, *Quasicommuting families of quantum Plücker coordinates*, Kirillov’s seminar on representation theory, 1998, pp. 85–108. MR1618743
- [Pen06] Robert Clark Penner, *Lambda lengths*, 2006.
- [Sco06] Joshua S. Scott, *Grassmannians and cluster algebras*, Proc. London Math. Soc. (3) **92** (2006), no. 2, 345–380. MR2205721
- [Zel00] Andrei Zelevinsky, *Connected components of real double Bruhat cells*, Internat. Math. Res. Notices **21** (2000), 1131–1154. MR1800992